ZEKE Spectroscopy of Complexes and Clusters

Klaus Müller-Dethlefs* and Otto Dopfer

Institut für Physikalische und Theoretische Chemie, Technische Universität München, Lichtenbergstrasse 4, D-85747 Garching, Germany

Timothy G. Wright*

Laser Spectroscopy Facility, Chemistry Department, The Ohio State University, 120 West 18th Avenue, Columbus, Ohio 43210

Received December 20, 1993 (Revised Manuscript Received May 3, 1994)

Contents

I. Introduction

In this review a number of complexes and clusters will be considered that have been studied by a new, high-resolution variant of photoelectron spectroscopy. Complexes considered include van der Waals species and hydrogen-bonded species. Photodetachment of an electron from a negative complex or cluster is another important area and has also been reviewed.

One of the most important areas where complexation and clustering occurs is in hydrogen-bonding systems. Hydrogen bonding is a subject that has received enormous attention over the years, owing to its ubiquity in biological systems.[1] The detailed study of hydrogen bonding in such systems is not straightforward, however, and attention has been focused on rather small systems in environments that are more amenable to interpretation by the chemist. The biggest successes have come from the study of 1:1 bonded complexes in molecular beams.[2,3] The complexes are easily formed in molecular jets by coexpanding a rare gas with a small percentage of the two monomers that are involved in the hydrogen bond. The large number of collisions that take place as the gas passes through a small hole and expands causes the complexes to be stabilized as they lose most of their internal energy. As well as preventing the complexes from dissociating, this cooling also serves to make the absorption spectra simpler. The link between gas phase studies and the liquid phase has been discussed by Kebarle[4] and Castleman and Keesee:[5] the work that has been performed on the direct photoelectron emission spectroscopy of aqueous solutions has been reviewed by Delahay.[6]

As an aid to understanding intermolecular forces[7] in more detail, van der Waals complexes are also of great interest. The simplest complexes are those that have a rare gas atom attached to a stable molecule, and these are also easily formed in molecular beams. Again, recent reviews have been published[8,9] on such species and the reader is directed to them and the references contained therein for further details.

Although numerous studies have been performed on neutral complexes, there are very few studies that have concentrated on cationic species. These species are of obvious importance as fundamental processes, such as solvation, depend on ionic species interacting with neutral molecules. The reason why there is a paucity of such studies is due to the difficulty of producing significant quantities of ionic complexes in the gas phase (although infrared spectroscopy of ions is an extremely active field[10]). The most widely applied technique to the study of ionic complexes in the gas phase is probably that of ultraviolet photoelectron spectroscopy (UVPES). It has been used to study a large variety of molecular complexes, usually using He I radiation, this work has been extensively reviewed recently[11,12] and so only an outline will be given here. It is also noted that X-ray photoelectron spectroscopy (XPS) has been used to probe the core levels of some molecular complexes, and this work has been reviewed by Hillier.[13]

In order to perform a UVPES study, the complex is generally in the gas phase, and in sufficient quantity to allow an adequate signal-to-noise ratio to be achieved. The formation is achieved in two ways: if the complex is strongly bound, then it may be possible to form it outside of the apparatus and leak it into the ionization volume; in the majority of cases, however, it is necessary to form the complex

0009-2665/94/0794-1845$14.00/0

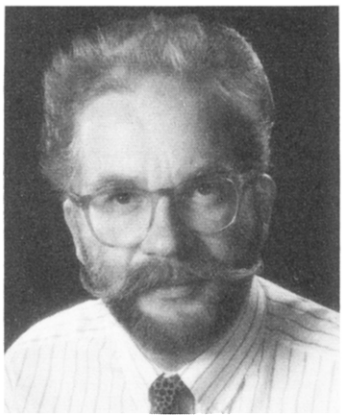

Dr. Klaus Müller-Dethlefs was born in Wilster in Germany in 1950. He was educated in chemistry and physics at the University of Göttingen and after completion of a thesis on combustion research (with H. Gg. Wagner) received his Diploma in chemistry in 1975. For his Ph.D. research he went to work in the group of F. J. Weinberg and A. Jones at the Imperial College of Science and Technology, University of London, UK. In 1979 he was awarded his Ph.D. from the University of London and also the Diploma of Imperial College for his thesis which involved an extensive study of soot formation in flames including the development of laser light scattering and laser induced fluorescence techniques. Having been awarded a postdoctoral research fellowship from the Deutsche Forschungsgemeinschaft, he then entered the area of nonlinear laser spectroscopy by working on coherent anti-Stokes Raman scattering (CARS) in the group of J. P. Taran at the Office National de Etudes et de Recherches Aérospatiales (ONERA) near Paris, France. In 1980 he joined the faculty at the Technische Universität München where he built up his own research group at the Institut für Physikalische und Theoretische Chemie (Director Edward W. Schlag). His most important research contributions stem from his invention of ZEKE spectroscopy in 1984. This discovery has led to a wide range of subjects being studied in his and, by now, many other groups in several countries. For his completed habilitation thesis he was awarded the Dr. rer. nat. habil. in 1991. His current position at the TU München is that of a nonpermanent Oberassistent. For his invention of ZEKE spectroscopy he has just been awarded the prestigious "Rudolf-Kaiser-Preis" by the "Stifterverband für die Deutsche Wissenschaft".

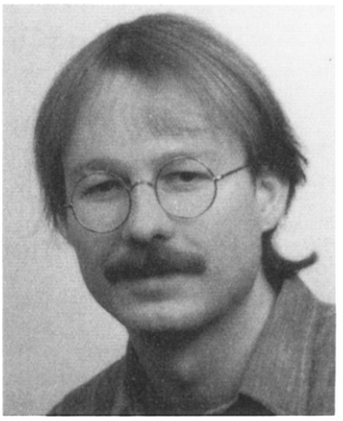

Otto Dopfer was born in Memmingen, Germany, in 1965. He received his Diploma in physics in 1991 from the Technische Universität München. Since 1990, he has been working in the research group of Klaus Müller-Dethlefs at the Institut für Physikalische und Theoretische Chemie, TU München, directed by Edward W. Schlag. His research interests include the spectroscopy of weakly-bound complexes in molecular beams to study weak intermolecular interactions under isolated conditions. His doctoral research—expected graduation by the end of 1994—includes the application of REMPI and ZEKE spectroscopy to various hydrogen-bonded phenol-containing complexes in order to obtain useful information about structure, dynamics, and intermolecular potentials of these species in neutral and cationic states.

Timothy Wright was born at R.A.F. Akrotiri (Cyprus) in 1965. He received his Ph.D. from the University of Southampton in 1991, under the supervision of J. M. Dyke, for his work on the application of conventional photoelectron spectroscopy and chemielectron spectroscopy to gas-phase metal oxidation reactions. In 1991 he was awarded a Royal Society Postdoctoral Fellowship to work at the Technische Universität München in the group of Dr. K. Müller-Dethlefs. He worked there until May 1993, on the application of ZEKE spectroscopy to various phenol complexes. He then was awarded a Postdoctoral fellowship from The Ohio State University to work in the group of Prof. T. A. Miller, developing a ZEKE spectrometer for the study of free radicals. In 1995 he will continue his research using ZEKE spectroscopy at Oxford University, collaborating with Dr. T. P. Softley, with the aid of a Lloyd's Tercentenary fellowship.

in situ, usually by coexpanding the components into the ionization volume. The major problem with a nonselective technique such as He I PES is that all the components of the reaction mixture contribute to the photoelectron spectrum. If the features are well separated in energy, then this causes no problem; but if the features are heavily overlapped, then large problems with interpretation ensue. To overcome this problem to some extent, spectral subtraction techniques[14] are used: with heavily-overlapped features this procedure is obviously difficult to perform completely reliably, especially if the complex's features are weak. Another disadvantage of the conventional PES technique is that, for the most part, the resolution is too poor to separate the individual features, characteristic of the intermolecular modes leading to broad spectral bands. What would aid matters significantly, and increase the accuracy of spectroscopic data and ionization energies, would be higher resolution.

Photodetachment spectroscopy (negative ion photoelectron spectroscopy) is also a very important area and has been reviewed by Lineberger and co-workers.[15] In this technique an electron is photodetached from a negative ion, usually making use of a laser. This technique thus gives information on the neutral species. Since the kinetic energy of the electrons is analyzed in the same way as in photoelectron spectroscopy, the same resolution restraints are present. Higher resolution would allow more detailed information to be derived about neutral species (spectroscopic data and electron affinities); many of the studied species are difficult to study by other methods.

The aim of this article is to review the large amount of work that has been performed recently using the technique of zero-kinetic-energy photoelectron (ZEKE) spectroscopy.[16-18] This technique will be described

in more detail in section II. In short, it is a form of photoelectron spectroscopy that allows an experimental resolution of less than 1 cm^{-1} to be achieved, which, for molecular complexes, means the widths of the peaks are only limited by unresolved rotational structure. This has allowed a number of workers to study *intermolecular* vibrations when molecular complexes are photoionized with laser radiation. The work has been concentrated in a number of areas and these divisions have been used as a basis for this review. They are the study of small molecular complexes, anionic complexes, organic molecules with inert ligands attached, and hydrogen-bonded complexes— in particular, phenol-containing complexes.

II. The ZEKE Technique

The ZEKE technique was developed in 1984 by Müller-Dethlefs *et al.*[19] and has revolutionized the field of photoelectron spectroscopy. The basis of the idea, as it was first formulated, was that if a laser accesses the ground (ro)vibronic ionization threshold of a neutral molecule, then a cation will be produced together with an electron with exactly zero kinetic energy (ZEKE), *i.e.* it is not moving. Now, if the laser is scanned through the higher-lying (ro)vibronic thresholds, then either *ZEKE electrons* will be produced, together with a rovibronically-excited ionic core, or kinetic electrons may be produced with an ion in a lower-energy state—with the proportion of each determined by the Franck–Condon factors (FCFs) for the ionization. While conventional photoelectron spectroscopy relies on the detection of the energy-analyzed kinetic electrons, the ZEKE technique detects the ZEKE electrons. This is achieved by using *delayed* pulsed-electric field extraction of the electrons from the ionization chamber, together with geometric discrimination. Since the kinetic electrons are, by definition, moving, then if a delay is employed between the time the laser is fired and when the extraction field is applied, the kinetic energy electrons will have moved away from the ionization volume (see Figure 1a). The ZEKE electrons will not have moved however, and if a time-of-flight analysis is performed, the ZEKE electrons will arrive at a different time and so may be selectively detected by electronic gating; the use of geometric discrimination prevents the majority of kinetic energy electrons from reaching the detector. This is the method that must be used for anions.

In 1988, Reiser *et al.*[20] discovered that, for neutral molecules, very long-lived, high-lying Rydberg states exist just below each ionization threshold. When the laser is scanned toward a threshold, these high-lying Rydberg states become populated and ionize when the pulsed electric field is applied (see Figure 1b). Since the Rydberg states will also not have moved from the ionization volume, this implies the electrons formed from their ionization will appear at the same time of flight as the ZEKE electrons. This poses no real problem, however, as the spectra obtained are very similar to the one that would have been obtained from the ZEKE electrons alone—for the purposes of this review both types of electrons will be called ZEKE electrons. [It should be noted however that some intensity effects can be observed in rotational

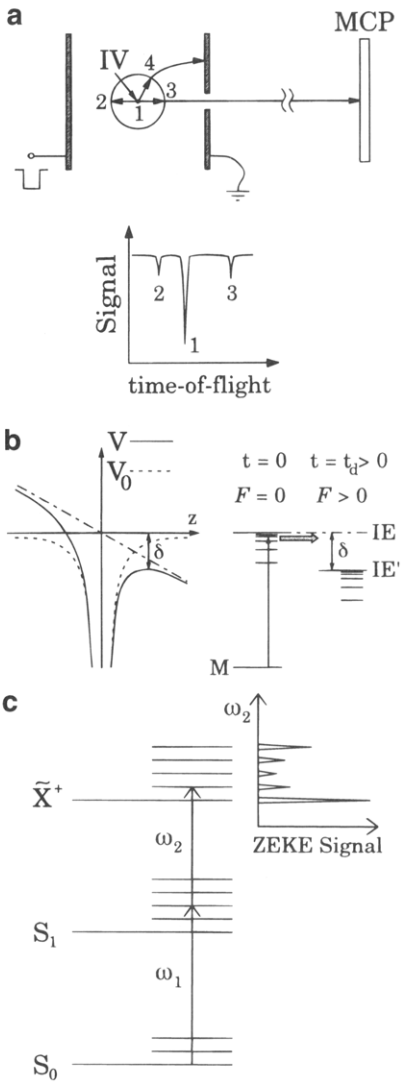

Figure 1. Part a shows the original ZEKE scheme. For $t = 0$, ZEKE electrons (1) and kinetic electrons (2–4) may be produced by the laser pulse at the ionization volume (IV) in a field-free region. A *delayed* extraction pulse ($t = t_d > 0$) extracts all electrons to the detector (MCP). ZEKE electrons (1) are detected selectively, and kinetic electrons are discriminated against them by time-of-flight gating (2 and 3) as well as by the steradiancy effect (4). Part b shows the pulsed-field ionization scheme. In the presence of an electric field F (the dotted and dashed line) the Coulomb potential V_0 (dotted line, here shown for the hydrogen atom) is modified by an additional linear potential, resulting in the final potential V (solid line). The field-free ionization energy (IE) is lowered by the Stark shift δ, given by the formula: $\delta = c\cdot\sqrt{F}$. Hence, by applying a *delayed* extraction field F at time t_d the high-lying, long-lived Rydberg states will be field-ionized. (M represents a neutral state of a molecule or cluster.) Part c shows a REMPI-ZEKE scheme. The first photon (ω_1) populates a (state and species) selected intermediate level. The photon energy of the second laser (ω_2) is scanned through the ionic levels and gives rise to peaks in the ZEKE signal whenever an ionic resonance is matched in energy.

structure, caused by Rydberg–Rydberg state interactions (for example in N_2[21]) and the work on these has been reviewed very recently.[22]] The longevity of the high-lying Rydberg states (now called ZEKE–Rydberg states) is presently understood as being due to the effects of small electric fields in the apparatus,[22–24] the presence of ions[25] and/or effects of higher multipole moments of the core.[26] The effects of these

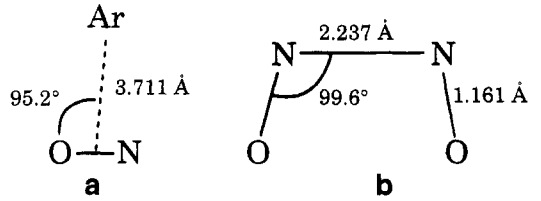

Figure 2. Sketch of the structure of (a) the neutral Ar–NO complex (geometry taken from ref 30) and (b) the neutral $(NO)_2$ complex (geometry taken from ref 46).

electric fields have also been investigated, for example, by Pratt on the ZEKE spectrum of NO[27] (exciting via the intermediate $A^2\Sigma^+$ resonant state), by Merkt on Ar[28] (via a one-photon process), and by our group for benzene[29] (exciting via the intermediate S_1 state).

In the majority of the ZEKE studies on neutral complexes, the ionization has been achieved in two steps (see Figure 1c for a diagram of the ionization scheme). The first step is the absorption of one photon which excites the molecule from its ground vibrational state to a *selected* (ro)vibronic level in an excited electronic state. This selection is not only specific to the energy state of the complex, but also to the molecular species, *i.e.* the complex may be *spectroscopically selected*. This is particularly advantageous as it allows a particular complex size (or conformer) to be chosen. (There may be many complexes of different sizes in the molecular beam, as well as the parent molecules themselves.) Once the selective excitation has occurred, another photon is absorbed; it is this second photon energy that is scanned in a typical ZEKE experiment. When the sum of the two photon energies matches the transition energy to a (ro)vibronic level in the ion, then ZEKE electrons will be produced and these will appear in the appropriate time gate. The variation of this gated signal as a function of the total laser energy gives rise to the ZEKE spectrum. The selection of the intermediate state has also been found to be advantageous since it allows the variation of the FCFs for the ionization step. In some cases, exciting through different levels has allowed the observation of some intermolecular (as well as intramolecular) modes that were not seen when exciting through other levels (*vide infra*).

III. Applications

a. Small Complexes

i. Ar–NO

The ground state neutral Ar–NO complex has been studied by a number of workers, with the definitive study being that of Howard and co-workers.[30] In this study, microwave and radiofrequency spectroscopy were used, which allowed the authors to derive an equilibrium geometry showing the molecule to be T-shaped, with a vibrationally-averaged deviation from pure T-shaped of 5.175° with the Ar atom closer to the nitrogen than to the oxygen atom (see Figure 2a). The vibrationally-averaged bond length—the distance between the Ar atom and the center of mass of the NO moiety—was derived as 3.711 Å. Of

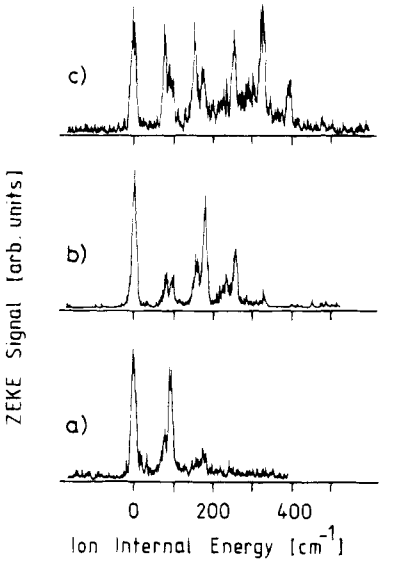

Figure 3. ZEKE spectra of NO–Ar via the $\tilde{C}$ state with zero (a), one (b) and two quanta (c) of the intermolecular stretch excited. (Taken from ref 31.)

particular note is that the orbital angular momentum is largely unquenched in the molecule, *i.e*, Λ is, by and large, a good quantum number, although strictly speaking there was a minimum energy orientation with the unpaired π-electron in the out-of-plane orbital. ZEKE spectra of Ar–NO were recorded in 1992 by Takahashi and Kimura.[31,32] The ionization energy was reached by exciting through the $\tilde{C}$ $^2\Pi$ state[33] of Ar–NO. The first laser was fixed on a particular vibronic level in the $\tilde{C} \leftarrow \tilde{X}$ transition and the second laser scanned through the ionization thresholds. The spectra obtained showed vibrational structure that was interpreted in terms of two vibrational series: nominally an intermolecular bend and an intermolecular stretch. The spectra (shown in Figure 3) were obtained when exciting through the $\tilde{C}$ state with zero, one and two quanta of the intermolecular stretch excited. (In the 2 + 1′ REMPI spectrum,[34] only the intermolecular stretch is excited.[35,36]) These gave spectra which showed different vibrational structure, indicative of the changing FCFs for the ionization step. The intermolecular bend series was measured to have a spacing of ~79 cm^{-1}, with that of stretch being measured as ~94 cm^{-1}. In fact, a more accurate analysis led to values for the harmonic vibrational frequencies of 80.3 and 99.6 cm^{-1} with anharmonic constants[37] of 1.0 and 3.55 cm^{-1} for the intermolecular bend and stretch, respectively. Franck–Condon calculations were performed in that work which made two significant approximations: first, harmonic oscillator potentials were used; and second, no account of the Duschinsky rotation[38] of the normal coordinates was taken. Within these assumptions, the intensity of the vibrational components in the 2 + 1′ REMPI spectrum were used to derive the changes in the geometry of the $\tilde{C}$ state. Although the signs of these changes were not known, it was reasonably assumed that the change would be negative, *i.e.* the bond length shortened. For the Ar–N–O bond angle, since no bend structure in the $\tilde{C} \leftarrow \tilde{X}$ transition was seen, the bond angle was assumed not to change. The geo-

Table 1. Experimental Geometries of the $\tilde{X}$, $\tilde{C}$, and $\tilde{X}^+$ States of Ar–NO

state	r_{N-O} (Å)	r_{Ar-N} (Å)	Θ_{Ar-N-O} (deg)
Ar–NO $\tilde{X}^2\Pi$	1.15077[a]	3.7064[b]	85.68[b]
Ar–NO $\tilde{C}^2\Pi$	1.062[a]	2.93	85.7[c]
Ar–NO$^+$ $\tilde{X}^{+1}\Sigma^+$	1.06322[d]	2.68	74.38 or 96.98[d]

[a] Huber, J. R.; Herzberg, G. *Molecular Spectra and Molecular Structure IV: Constants of Diatomic Molecules*; van Nostrand Reinhold: New York, 1979. [b] From ref 30. [c] Assumed to be the same as that of the $\tilde{X}^2\Pi$ state since there was no bend vibration seen in the (2+1′) REMPI spectrum. (See ref 31.) [d] In ref 31 a negative decrease of the bond angle was assumed; the results of ref 39 suggest an increase of the bond angle on ionization and hence support the higher value.

metric parameters for the $\tilde{C}$ state were then used, together with the experimental intensities in the ZEKE spectrum, to derive geometric parameters for the ground cationic state. Again, since the absolute values of the changes could not be determined, the change in the bond length was assumed (again reasonably) to be negative. At this point it is necessary to point out that some errors in the use of the complex geometry occurred in ref 31—these errors have been outlined and corrected.[39] The ground state geometry and the derived geometries of the $\tilde{C}$ and $\tilde{X}^+$ states are given in Table 1. [Here, a "+" is appended to the label of the term symbol for a cation (the common use of D_0 is ambiguous, owing to its use for a dissociation energy); for anions a "−" is appended.] Two *ab initio* calculations on the Ar–NO$^+$ complex have been published recently.[39,40] The first of these[40] used a so-called "modified CIPSI" approach which was size consistent (an important consideration in dealing with the energies of molecular complexes).[41] The paper contained contour plots of the potential energy surface, which seemed to suggest that the minimum energy of the Ar–NO$^+$ complex was at a bond angle of *ca.* 90°—a result in agreement with a recent calculation[39] that used rather large basis sets and the MP2 level of theory.[42] The experimentally-derived bond angle would agree well with the calculated values, if the derived change in bond angle was taken to be positive rather than negative (as was taken in ref 31). The calculated bond lengths of the two studies disagreed somewhat, however, with the first study[40] disagreeing with the experimental bond length, whereas the second study[39] supported it. A summary of the experimentally-derived geometries of the different states of Ar–NO are given in Table 1.

The difference between the ionization energy of the Ar–NO complex and the NO molecule is equal to the difference between the D_0 values of the neutral and cationic Ar–NO ground states. The ionization energy of NO$^+$ is known very accurately from both Rydberg series extrapolations[43] and ZEKE spectroscopic studies.[20] The D_0 value for the ion was reevaluated[39] as 920 ± 20 cm^{-1} using the adiabatic ionization energy of Ar–NO[31] (73869 ± 6 cm^{-1}). (Note that the ionization energy from the ZEKE study was *higher* than that obtained *via* the REMPI-PES study,[35] but this was attributed to instrumental effects present in the earlier study.)

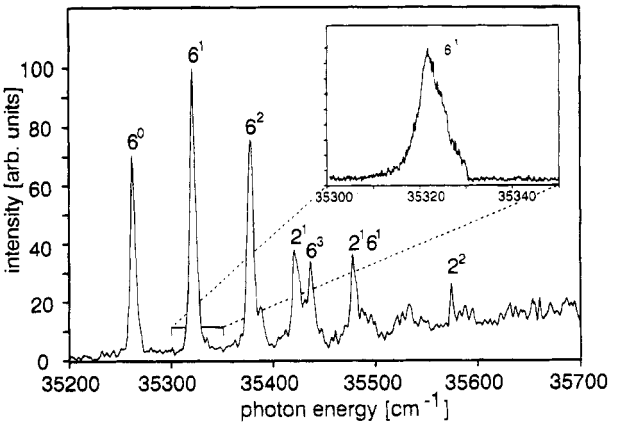

Figure 4. Nonresonant one-color, two-photon ZEKE spectrum of the NO dimer. The inset shows a high accuracy scan of the rotationally broadened 6^1 band. (Taken from ref 51.)

ii. $(NO)_2$

The NO dimer has been the subject of a number of experimental studies, and its cation has been detected in the Earth's atmosphere.[44] The geometric structure has been determined very accurately from electric resonance spectroscopy and microwave studies.[45,46] A complete description of the work prior to 1981 has been given in ref 45. Both infrared[47] and Raman[48] spectroscopic studies have been performed, and very recently, Fourier transform infrared spectroscopy was used to follow the formation of the NO dimer, formed from NO diffusing through a nitrogen matrix.[49] An *ab initio* study at the configuration interaction (CI) level has been performed by Ha,[50] in which single point calculations were carried out with the experimental geometry of the ground state neutral being employed. The study of direct interest here is the one-color, two-photon, *nonresonant* ZEKE spectrum recorded by Fischer *et al.*[51] The spectrum (shown in Figure 4) demonstrates a progression of three quanta of the ν_6 mode which, by comparison with the earlier infrared and Raman spectroscopic studies, was assigned to a torsional mode (a_2 symmetry). This implies that the $(NO)_2^+$ species has C_2 symmetry (*gauche* out-of-plane), in contrast to the C_{2v} symmetry of the ground state neutral species (see Figure 2b). The ν_2 mode also appeared in the ZEKE spectrum, albeit not as prominently as the ν_6 mode; the ν_2 vibration is probably the symmetric bend, leading to the conclusion that the molecule either closes together in a scissor action, or perhaps opens. It would be useful to perform *ab initio* calculations on the cationic species. The N–O symmetric stretch was also seen in the ZEKE study and yielded a value of 2090 cm^{-1} (Table 2), a result consistent with the expected bond order of the cation of $2^3/_4$; thus, the charge appears to be equally shared between the NO moieties.

The adiabatic ionization energy of $(NO)_2$ was measured as 70350 ± 5 cm^{-1} which was in close agreement with previous determinations, most notably the value of 8.746 eV obtained by Ng *et al.*[52] from photoionization efficiency measurements. Again, by comparison with the known ionization energy of NO and the known binding energy of the neutral

Table 2. Vibrational Frequencies of the NO, $(NO)_2$, and $(NO)_2^+$ Ground States

vibrational symmetry	qualitative description	neutral	ion
	NO		
Σ_g^+	ν_{NO}	1876[a]	2344[a]
	$(NO)_2$		
A_1	ν_{NO}(sym)	1860[b]	2090[c]
	δ_{NNO}(sym)	263[b]	323[c]
	ν_{NN}	170[b]	
B_1	ν_{NO}(asym)	1789[b]	
	δ_{NNO}(asym)	198[b]	
A_2	τ	88[b]	118[c]

[a] Huber, J. R.; Herzberg, G. *Molecular Spectra and Molecular Structure IV: Constants of Diatomic Molecules*; van Nostrand Reinhold: New York, 1979. [b] From the summary presented in ref 47. [c] From ref 51.

$(NO)_2$ complex (787 cm^{-1}),[47] it was possible to derive the binding energy of the ionic complex as 4979 cm^{-1}.

iii. Al_2

Harrington and Weisshaar applied the technique of ZEKE spectroscopy to the aluminum dimer.[53] Aluminum clusters were produced in the throat of a molecular expansion by laser ablation of an aluminum target rod. The subsequent expansion (in helium) cooled the clusters considerably and Al_2 was selectively excited by using the (1−0) and (2−0) vibrational components of the $F^3\Sigma_g \leftarrow X^3\Pi_{u0}$ transition, previously reported by Cai *et al.*[54] (The parity of the F state is not known.[55]) A second laser was scanned through the ionization thresholds of the ions, using a delay of 2 μs between the laser pulses and the extraction of the electrons by a pulsed electric field. This gave rise to a vibrationally-resolved spectrum with 15 cm^{-1} wide peaks (some of the width will have been due to unresolved rotational structure). The ZEKE spectrum was interpreted in terms of a progression of the vibrational frequency of the ion. This allowed the determination of an $\bar{\omega}_e$ value of 178 ± 8 cm^{-1} and an $\bar{\omega}_e x_e$ value of 2 ± 2 cm^{-1}. The first member of the progression was taken as the adiabatic ionization energy (AIE) and this gave a value of 5.989 ± 0.002 eV (the same ionization energy was obtained from both the (1−0) and (2−0) intermediate states). There was quite remarkable agreement of the *ab initio* results from Sunil and Jordan[56] (AIE = 5.92 eV) and Bauschlicher *et al.*[57] (AIE = 5.90 eV). The later study also calculated the vibrational frequency of the ion as 169 cm^{-1}, in excellent agreement with experiment. An intriguing result from the experimental study concerns the relative dissociation energies of the neutral and cationic ground states of the aluminum dimer. Since the difference in the ionization energies of the aluminum atom and the aluminum dimer is equal to the difference in the D_0 values for the neutral and cationic ground states of the dimer, and since the ionization energy of aluminum atom is 5.986 eV,[58] this means that the cation and neutral states have identical binding energies to within 5 meV.[53] The neutral aluminum dimer is bound by half a σ-bond and half a π-bond with the π-electron being lost on ionization. [The outer electronic configuration of the neutral dimer is $(3p\sigma_g)^1$-$(3p\pi_u)^1$.] This would imply that the π-electron is essentially nonbonding: a result contrasted by the fact that the vibrational frequency in the neutral[59] is 278 cm^{-1} with a bond length of 2.701 ± 0.002 Å, *cf.* the cation vibrational frequency noted above. The dissociation energy of the neutral X state was derived as 1.34 ± 0.06 eV from a high-resolution spectroscopic study.[59]

iv. Xe_2

The rare gas dimers have been the subjects of a great number of experimental and theoretical studies,[1,60] mainly because they represent one of the simplest van der Waals species. The most recent theoretical study by Ma *et al.*[61] calculated the ionization energies of all R_1R_2 species (R_1, R_2 = He, Ne, Ar, and Kr), using the so-called *Gaussian 2*[62] approach. The only ZEKE spectroscopic study has come from the White group.[63] In this study, one-photon ionization of Xe_2, formed by supersonic expansion of Xe through a 20 μm nozzle, was used. The ionizing radiation was produced by four-wave sum mixing.[64] The ZEKE spectrum showed a long progression of the internuclear vibration of the Xe_2^+ A^+ $^2\Sigma_u^+$ state: the adiabatic ionization energy was not observed however, owing to poor FCFs in that energy region. Studies with isotopically-enriched samples were also performed. Analysis of the spectrum led to an assignment of the vibrational structure, which indicated that the lowest vibrational feature corresponded to $v' = 56$ in the ion. The harmonic vibrational frequency $\bar{\omega}_e$ was determined as 114.7 cm^{-1} with $\bar{\omega}_e x_e$ equal to 0.417 cm^{-1}; the T_e value was 90312 cm^{-1}. The adiabatic ionization energy was derived as 90360 ± 70 cm^{-1}, but it was noted that this was inconsistent with some previous experiments: in particular a MPI-PES study by Pratt *et al.*[65] and a photoionization efficiency measurement[66] by Ng and co-workers. This discrepancy was attributed to the poor FCFs in the region of the ionization threshold. As suggested,[66] exciting via an intermediate state in a two-color ZEKE experiment could lead to a more unambiguous determination of the ionization threshold, since better FCFs can be expected by a good choice of the resonant intermediate state. Finally, the dissociation energy of the A^+ state, D_0, was determined to be 7660 ± 70 cm^{-1}. As well as the A^+ state, the B^+ and C^+ states were also investigated in the ZEKE study. For the B^+ state it was not possible to elucidate completely the vibrational assignment, but the dissociation energy, D_0, could be estimated as ≥1230 cm^{-1}; the vibrational frequency $\bar{\omega}_e$ was found to be ≥45 cm^{-1}. For the C^+ state, no such problem occurred and the dissociation energy, D_0, was determined as 442 ± 2 cm^{-1}; the vibrational frequency $\bar{\omega}_e$ was determined as 23.1 cm^{-1}.

b. Anions

The study of anions by ZEKE spectroscopy poses significant problems since the pulsed-field ionization variant of the ZEKE technique shown in Figure 1b may not be used (since the requisite Rydberg states do not exist), and in fact, electrons just above threshold within a very small energy range are detected (see Figure 1a). This, in turn, implies that

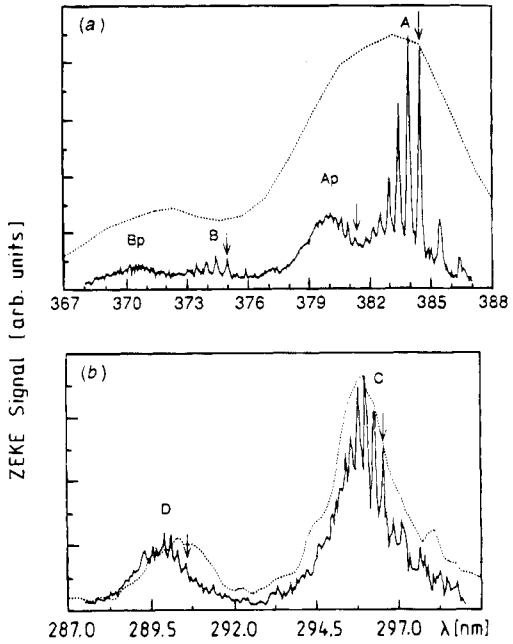

Figure 5. Threshold photodetachment (ZEKE) spectrum of I^-–CO_2 (solid lines) and conventional photodetachment spectrum (dotted lines). The arrows indicate the band origins. See text for details. (Taken from ref 74.)

significantly more care must be taken to shield the ionization region from stray electric and magnetic fields. Neumark and co-workers first applied the ZEKE method to photodetachment spectroscopy[67] and have been very active in this field, successfully performing studies on carbon clusters, silicon clusters, transition-state complexes, and the I^-–CO_2 complex. Each of these applications will be considered in the following subsections. The other main area of application is to metal clusters. These have been performed in the group of Kaldor and are currently also being developed in the Jülich group.[68] What is perhaps surprising is the speed of these groups in recognizing the utility of the ZEKE technique. Photodetachment spectroscopy of anionic clusters is a very active field of research. It is a very useful technique as mass selection of the (charged) clusters may be achieved, and then the information gained from the photodetachment spectrum gives direct information on the neutral species.

i. I^-–CO_2

Work using conventional photodetachment spectroscopy has been performed on a number of iodine clusters, such as I^-–$(H_2O)_n$,[69,70] I^-–$(CO_2)_n$,[71,72] and I^-–CH_3I.[73] A ZEKE spectroscopic study[74] has been performed, and it is on this study that attention will be focused here, especially on the gain in information that is obtained in the increasing resolution of the reported studies on the I^-–CO_2 complex[71,72,74] (see Figure 5).

In the first conventional photodetachment study,[71] clusters were formed by coexpanding CO_2 with halogen-containing compounds, both of which were entrained in argon, through a pulsed nozzle. The negatively-charged clusters were produced by crossing the molecular expansion with a 1000 eV electron beam; the clusters are then mass separated and clusters of the selected mass enter the photodetachment spectrometer. Photodetachment was achieved by the fourth harmonic of a Nd:YAG laser (4.66 eV), and the photoelectrons were kinetic energy analyzed by a magnetic bottle-type spectrometer:[75] the resolution achieved was 50 meV (*ca.* 400 cm^{-1}). For the 1:1 complex only two bands were observed in the photodetachment spectrum, corresponding to the two spin–orbit components of I, shifted slightly owing to the complexation. In fact I^-–$(CO_2)_n$ clusters with $n = 0-7$ were studied in this work, giving a picture of the changes in binding energy of the cluster as the number of solvent molecules increased. In a slightly later study, Neumark and co-workers[72] again studied I^-–$(CO_2)_n$ clusters, $n = 1-13$. The methods of generation, photoionization, and kinetic energy analysis of these clusters were very similar to the previous study; however, a linear time-of-flight electron analyzer was used, giving a resolution of ~11 meV (*ca.* 90 cm^{-1}). This increase in resolution allowed some vibrational structure on each of the spin–orbit components in the I^-–CO_2 photodetachment spectrum to be achieved (see Figure 5, dotted lines). The spacing in this progression was determined to be 665 ± 90 cm^{-1} and was assigned to the bending mode (ν_2) of the CO_2 moiety. This clearly demonstrated that there was a change in ∠OCO upon photodetachment of the anionic cluster. It was reasonably argued that, since the van der Waals interaction in the neutral state is weak, the distortion of the linear CO_2 geometry is in the anion (the I^-–CO_2 cluster is roughly T-shaped with the I^- bound to the carbon atom: a result consistent with charge transfer from I^- to CO_2). A simple Franck–Condon analysis led to the derivation of a OCO bond angle of *ca.* 175°.

Owing to the increased resolution of the ZEKE spectroscopic study[74] (Figure 5, solid lines), a more in-depth look at the bonding in the I–CO_2 cluster was needed. The neutral cluster is formed by the combination of $I(^2P_{1/2})$ and $CO_2(\,^1\Sigma_g^+)$ or $I(^2P_{3/2})$ and CO_2 ($^1\Sigma_g^+$). By analogy with a rare gas–I complex, three states are possible, corresponding to $\Omega = {}^1/_2$ and ${}^3/_2$ derived from the lower spin–orbit component of I and the $\Omega = {}^1/_2$ state derived from the upper spin–orbit state—they are the $\tilde{X}^2\Sigma_{1/2}$, the $\tilde{A}^2\Pi_{3/2}$, and the $\tilde{B}^2\Pi_{1/2}$ states. In that work,[74] these states were denoted X ${}^1/_2$, I ${}^3/_2$, and II ${}^1/_2$, respectively. The complexes were created in the same way as in the previous photoelectron study, but this time photodetachment was achieved by a tunable dye laser which was scanned through the ionization thresholds of interest; the ZEKE electrons were detected after a delay of 150–200 ns. The resolution achieved in this instrument was 0.3 meV (*ca.* 2.5 cm^{-1})—obviously a great improvement over the two earlier experiments. The spectra (shown in Figure 5) show six main features labeled A, Ap, B, Bp, C, and D. These features were assigned as follows: A, Ap, and C to transitions from the ground state of the anion into the $\nu_2 = 0$ levels of the $I(^2P_{3/2})$–CO_2 [X ${}^1/_2$; I ${}^3/_2$] and $I(^2P_{1/2})$ [II ${}^1/_2$]; B, Bp, and D to the corresponding transitions with $\nu_2 = 1$. The structure in each of these bands (not resolved in the earlier studies, see for example the dotted curve in Figure 5) had separations of *ca.* 30 cm^{-1} and this was assigned to a progression of the van der

Waals C—I stretching mode (denoted ν_3). Analysis of the hot band structure gave a value of 64 cm^{-1} for the same vibration in the anionic complex.

ii. Metallic Clusters

A number of metallic anionic clusters have been studied[76-78] by Gantefor *et al.* They produce the metal clusters by laser vaporization of a metal target in the throat of a molecular expansion, and the mixture of anions, cations and neutrals pass through a skimmer. The anions are accelerated and this results in the separation of clusters of different mass. A particular mass is then irradiated in a ZEKE photodetachment experiment. The first study looked at the gold dimer and the silver trimer.[76] For Au_2^- the results showed a progression in the vibrational frequency of the neutral, leading to its determination as 146 cm^{-1}. There were also hot bands in the spectrum which led to the derivation of the ground state anionic vibrational frequency as *ca.* 188 cm^{-1}. The 0—0 band in the ZEKE spectrum was taken as the electron affinity and led to a value of 1.9400 ± 0.0005 eV. A FCF analysis led to the derivation of the vibrational temperature of the sample gas as 165 ± 30 K. For Ag_3^- only one peak was observed in the ZEKE spectrum.[77] At first sight this may be a little surprising as the geometry of Ag_3^- is linear, whereas the geometry of Ag_3 is an equilateral triangle. However, there is a linear state of Ag_3 that lies 0.05 eV above the triangular state,[79] and it is detachment to this state that was thought to be responsible for the ZEKE spectrum. The gold hexamer (Au_6^-) was also studied[78] and the ZEKE spectrum showed a progression of a vibration of 107 cm^{-1} which was also present in the electron total yield spectrum. These studies demonstrate that fundamental information on metal clusters can be accurately determined from the ZEKE photodetachment spectra—the mass selectivity possible for the anions, together with the sensitivity of the ZEKE scheme combine to provide a powerful tool for the gaining of information on the neutral species, which is difficult to obtain by other means.

iii. Carbon and Silicon Clusters

The large bulk of information on metal and semiconductor clusters has been comprehensively reviewed recently by a number of authors,[80] as has the chemistry of carbon clusters.[81]

Carbon Clusters. There has been a huge amount of work performed on carbon clusters. A recent review[81] details the work up until April 1989. For good overviews of the work performed until mid 1992, the reader is referred to the introductions of the two papers by Neumark and co-workers.[82,83] High-resolution infrared spectra of the neutral species have been recorded by Saykally, Amano, and Bernarth and their co-workers—see references quoted in ref 83. In recent photodetachment studies, carbon clusters were produced by laser vaporization of graphite in the throat of a molecular expansion. These were then collided with electrons downstream to obtain the negative clusters. Mass selection can then be performed before the experiment is carried out. The size of clusters can be controlled to some extent by varying the power and the wavelength of the ablating laser source.[84] The most recent conventional photodetachment spectroscopy of carbon clusters has been from the groups of Smalley and Neumark. The studies by Yang *et al.*[85,86] used photodetachment by ArF and F_2 excimer lasers. The resolution in these studies was rather poor. However, they did have the advantage that a large range of negative carbon clusters could easily be studied: C_n^- (n = 2—84). A slightly later study,[82] obtained a significantly better resolution of *ca.* 10 meV (80 cm^{-1}) in a study which concentrated on the C_n^- (n = 2—11) clusters. Photodetachment was performed with the third and fourth harmonics of a Nd:YAG laser. Accurate electron affinities were obtained in this work and compared with *ab initio* results, where they were available. The agreement in the majority of cases was quite good; as was the agreement with previous results.

In the rest of this subsection, attention will be focused upon the C_5^- and C_6^- clusters. An important point to note here is that the photodetachment spectra, if well enough resolved, can lead to observation of vibrational structure attributable to totally symmetric modes, these are not observable using the technique of high-resolution infrared absorption, mentioned above. The (linear) C_5^- spectra[82] (noted as corresponding to the $X^1\Sigma_g^+ \leftarrow X^{-2}\Sigma_g^+$ photodetachment, but this assignment is altered in the ZEKE spectroscopic study, *vide infra*) were interpreted in terms of both totally and non-totally symmetric vibrations and the assignment was based on *ab initio* results. For C_6^-, the structure is thought to be linear, but the ground state geometry for the neutral cluster is a point of controversy; it is certainly true to say that there are two structures very close in energy. By assuming that the detachment process is from linear to linear structures, then the interpretation of the photodetachment spectrum was made, again by comparison with *ab initio* results. For both C_5^- and C_6^-, "tails" in the spectra were suggested as being due to transitions from cyclic states of the C_5^- and C_6^- species. For the two specific clusters mentioned, ZEKE photodetachment experiments have also been performed by Neumark and co-workers, with resolutions of ≤10 cm^{-1} and these will now be reviewed.

For C_5^-, a very clear vibrational structure was obtained.[87] The dominance of an intense peak at threshold (also seen in the lower resolution study[82]) indicated that the change in geometry between the anion and the resulting neutral cluster was small. Thus, since C_5 was known to be linear, this result implied that the ground state of the C_5^- anion was also linear. This intense peak at threshold was found to be split by 22 cm^{-1} into a doublet, and this was interpreted in terms of spin—orbit splitting in the $X^{-2}\Pi_u$ ground state. The electron affinity was accurately determined to be 2.853 ± 0.001 eV. Four vibrational fundamentals were identified, and these were assigned by comparison with (scaled) harmonic frequencies calculated by Raghavachari and Binkley.[88] The broader structure in the spectrum, to higher energy, was assigned to an excited electronic state of C_5. Considering the electronic configuration of C_5^- as $\sigma_g^2\sigma_u^2\pi_g^4\pi_u^1$ and the interesting point that

only *s*-wave electrons can be seen in a photodetachment spectrum,[89] then, since it has been shown[90] that *s* waves can only occur (under $D_{\infty h}$ symmetry) when an electron is photodetached from a π_u or σ_u orbital, it was concluded that the excited state must arise from the removal of the σ_u orbital, giving a $^3\Pi_g$ state. The broadness of the spectrum was interpreted in terms of unresolved spin–orbit structure. It was noted, however, that some detailed (multireference configuration interaction) *ab initio* calculations had predicted a $^3\Pi_g$ state at 2.56 eV,[91] significantly higher than the experimentally-determined separation of 0.26 eV. The possibility that this higher-energy feature was due to autodetachment from a metastable state of C_5^- was considered but discounted as kinetic electrons originating from autodetaching levels should have been discriminated against by the ZEKE detection scheme. Additionally when a total electron distribution was recorded no additional features owing to this complex could be seen: this discrepancy remains unresolved.

For the C_6^- work,[83] the resolution had been increased even further to 3 cm^{-1}. The spectrum (as for C_5^-) was dominated by an intense peak at threshold, again indicating that the geometries of the anion and neutral states are similar. The doublet structure in the spectrum was interpreted as being due to the spin–orbit splitting in the anion: the anionic electronic state is $^2\Pi_u$, whereas the ground state of the neutral is $^3\Sigma_g^-$. Hence, the splitting of 29 cm^{-1} is attributable to the anion. The electron affinity of C_6^- (taken as being the first peak in the ZEKE spectrum) was derived as 4.180 ± 0.001 eV. The interpretation of the vibrational structure was in terms of three symmetric vibrations (two of whose values were in poor agreement with the *ab initio* results of Martin *et al.*,[92] whose calculations were performed at the MP2/6-31G* level of theory). The observation of three totally symmetric modes also argued against a cyclic geometry (suggested previously)[88] for these states, since this geometry would only be expected to have two totally symmetric modes. A simple Franck–Condon analysis was performed in order to ascertain the geometry change on going from the anion to the neutral. This analysis only assumed geometry changes along the totally symmetric coordinates and the simulated spectrum fitted the experimental spectrum well. Although the magnitudes of the changes in geometry along the particular normal coordinates could be derived, the absolute sign could not. An absolute geometry was obtained by comparison with *ab initio* calculations of the geometries of the neutral and anionic states. Autodetaching levels were also found in this work[83] (*i.e.* excited anionic levels that are above the neutral ground state), but this will not be discussed here, except to note that the origin of this state is 43 cm^{-1} *below* the photodetachment threshold, with the autodetachment occurring from vibrationally excited levels.

Silicon Clusters. *Si_2^-*. The smallest anionic silicon cluster, the Si_2^- species, has been studied by photodetachment spectroscopy by a number of groups. The first such study was that of Nimlos *et al.*,[93] where silicon clusters were produced by a dc electric discharge through a mixture of silane and ammonia. Mass selection was performed with a Wien filter and the Si_2^- ions were photodetached with an Ar ion laser operating at either 488 or 457.9 nm. Electron kinetic energy analysis was performed by hemispherical electrostatic analyzers with a resolution of *ca.* 20 meV, with calibration of the energy scale being achieved by photodetachment spectroscopy of OH^-. The silicon dimer has an outer configuration of $(\sigma_g)^2(\pi_u)^2$ which gives rise to $^3\Sigma_g^-$, $^1\Delta_g$, and $^1\Sigma_g^+$ electronic states, but there are low-lying electronic states arising from the configurations $(\sigma_g)^1(\pi_u)^3$ [$^3\Pi_u$ and $^1\Pi_u$] and $(\sigma_g)^0(\pi_u)^4$ [$^1\Sigma_g^+$]. The anion has a $(\sigma_g)^1(\pi_u)^4$ outer configuration, giving rise to a $^2\Sigma_g^+$ electronic state, with a low-lying $^2\Pi_u$ state arising from the $(\sigma_g)^2(\pi_u)^3$ configuration. This ordering of the electronic states was confirmed by MCSCF+CI calculations.[93] The assignment of angularly-resolved photodetachment spectra obtained in that work[93] was based on the results of these calculations (energy separations and vibrational frequencies) to a large extent. The ground state of the neutral molecule is the $X^3\Sigma_g^-$ state as had been determined earlier by Douglas[94] and later confirmed by ESR spectroscopy.[95] The photodetachment spectra in the work of Nimlos *et al.*[93] were recorded at angles of 0° and 90° and these gave rise to significantly different intensity patterns in the spectra for the four peaks seen. These two spectra were used to determine the anisotropy parameter β for each of the three peaks and this in turn was used to infer the nature of the orbital to which each peak corresponded. Some of the assignments of the peaks in the spectrum were not clear, but further use of *ab initio* calculations clarified the situation to give a consistent interpretation. The electron affinity was derived as 2.199 ± 0.012 eV and attributed to the Si_2 ($X^3\Sigma_g^-$) + e^- ← Si_2^- ($^2\Pi_u$) photodetachment. The separation between the Si_2 ($A^3\Pi_u$) and the Si_2 ($X^3\Sigma_g^-$) states was derived as 0.053 ± 0.015 eV and the separation between the Si_2^- ($^2\Pi_u$) and the Si_2^- ($^2\Sigma_g^+$) states was derived as 0.117 ± 0.016 eV, with the $^2\Pi_u$ state concluded to be lower—*this is in contrast to the most recent ZEKE results* (*vide infra*), where the $^2\Sigma_g^+$ state is concluded to be the ground state by 0.025 ± 0.010 eV.

Conventional photodetachment and ZEKE spectroscopic studies were performed on Si_2^- by Neumark and co-workers[96,97] (the second reference[97] contains a reassignment of some of the spectral features reported in the first). The conventional photodetachment spectrum and the corresponding ZEKE spectra are compared in Figure 6. (The labeling in the ZEKE spectrum has been modified to agree with the recent reinterpretation).[97] Considering first the conventional photodetachment spectrum (Figure 6a), the spectrum may be divided into two sections: the section with electron kinetic energy ranging from 1.0 to 1.5 eV and the section from 0.5 to 0.9 eV. The higher kinetic energy region is the same region as that studied by Nimlos *et al.*,[93] although features e, E, and F were not seen owing to the lower energy photodetaching radiation used; additionally, features d and D were not resolved. The photodetachment spectrum was recorded with two different laser

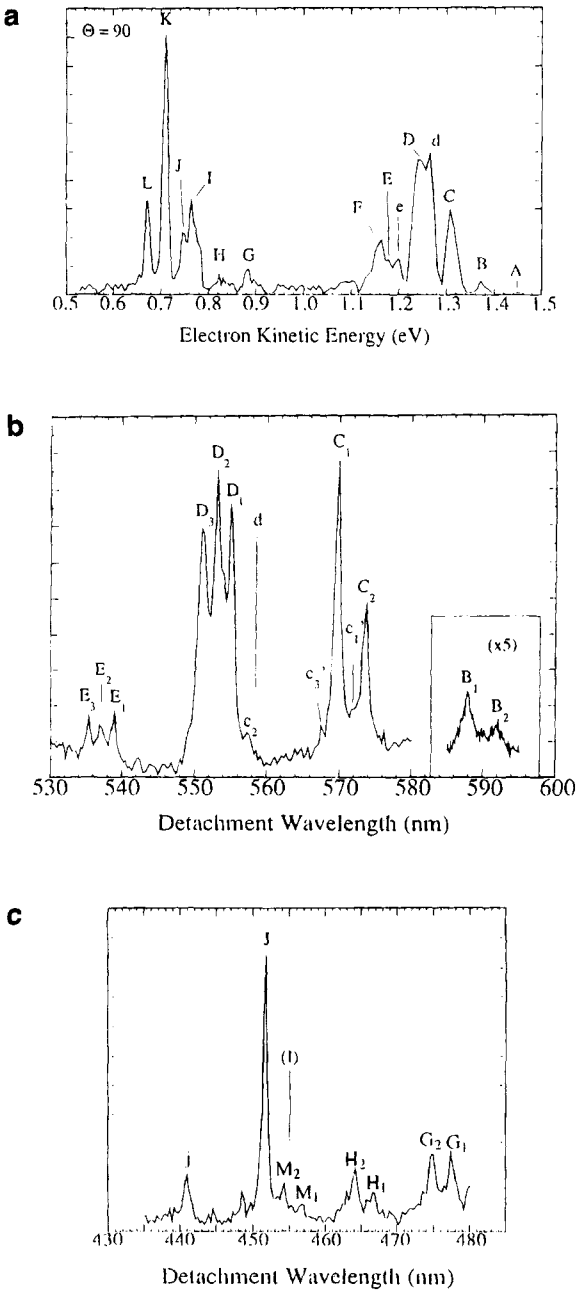

Figure 6. (a) Photodetachment spectrum of Si_2^- with laser polarization perpendicular to the direction of electron detection (the detachment wavelength is 355 nm) (taken from ref 97); (b) ZEKE spectrum of Si_2^- showing transitions to the triplet states of Si_2 (taken from ref 97); (c) ZEKE spectrum of Si_2^- showing transitions to the singlet states of Si_2 (taken from ref 97).

polarizations (parallel and perpendicular to the electron detection direction)—the spectrum in Figure 6a is the one with the laser polarization perpendicular to the electron detection direction. All features in the spectrum shown in Figure 6a are also in the photoelectron spectrum with the laser polarization parallel to the electron detection direction (not shown here) although there are intensity differences: notably features D and J are much stronger in the spectrum recorded with the laser polarization parallel to the electron detection direction, whereas feature K is much weaker and features e and d are not evident in the parallel laser polarization spectrum. By looking at the changes in intensities of various features in the two spectra under different polarization schemes, the different contributions of vibrational and electronic transitions to the photodetachment spectrum could be distinguished. The ZEKE spectrum corresponding to the high kinetic energy region of the conventional photodetachment spectrum (shown in Figure 6b) showed it to consist of the transitions to the triplet neutral states. It is important to note here that (as with photoelectron spectra) only photodetachment (ionization) that involves one-electron processes can occur, in general. Thus, the transition from the $^2\Sigma_g^+$ anionic state to the $X^3\Sigma_g^-$ state of the neutral molecule, is forbidden. Also, only *s* waves are observable in the ZEKE spectrum for anions (*vide supra*) and so the transitions seen in the ZEKE spectrum here must correspond to π_u photodetachment, and σ_g photodetachment is not observable (under $D_{\infty h}$ symmetry). Thus, it was possible for Neumark and co-workers to assign the features that were present in the conventional photodetachment spectrum, but not present in the ZEKE spectrum, to π_u photodetachment; the features that were present in both spectra could be assigned to σ_g photodetachment. Thus, the triplets D and E were assigned to the following transitions:

$$\text{D:} \quad A^3\Pi_\Omega\,(v'=0) \leftarrow {}^2\Sigma_g^+$$

$$\text{E:} \quad A^3\Pi_\Omega\,(v'=1) \leftarrow {}^2\Sigma_g^+$$

Peaks d and e (not seen in the ZEKE spectrum in Figure 6b) were assigned to the $^3\Pi_u \leftarrow {}^2\Pi_u$ transitions. Peaks B and C, that appear as doublets (splitting 122 ± 10 cm^{-1}) were assigned to the $X^3\Sigma_g^- \leftarrow {}^2\Pi_{\Omega u}$ ($v'' = 1$) and $X^3\Sigma_g^- \leftarrow {}^2\Pi_{\Omega u}$ ($v'' = 0$) photodetachment, respectively.[98] The very weak feature A (doublets not resolved) in the conventional photodetachment spectrum was assigned to the $X^3\Sigma_g^- \leftarrow {}^2\Pi_{\Omega u}$ ($v'' = 2$) transition. The low kinetic energy region of the conventional photodetachment spectrum in Figure 6a (the corresponding ZEKE spectrum is shown in Figure 6c) was assigned to transitions to singlet states of the neutral molecule. These were assigned by again noting that only one-electron photodetachment is allowed, only *s* waves will be detected in the ZEKE spectrum, and any doublet peaks that are observed must have originated from the $^2\Pi_u$ anionic state. In this way, the series of three sets of double peaks (G, H, and M) were assigned to the $a^1\Delta_g \leftarrow {}^2\Pi_{\Omega 1/2}$ photodetachment, with $v'' = 0$, 1, and 2. The features J and j are then assigned to the last remaining *s*-wave photodetachment, the $b^1\Pi_u \leftarrow {}^2\Pi_u$ transition, with $v'' = 0$ and 1. Finally, peak K was tentatively assigned to the *p*-wave photodetachment $c^1\Sigma_g^+ \leftarrow {}^2\Sigma_g^+$. Peaks F and L remain unassigned, although it was noted that they probably belong to transitions to different spin multiplets of the same electronic state. The state ordering for the anion was determined and gave the $^2\Sigma_g^+$ as the ground state, with the $^2\Pi_u$ state lying 0.025 ± 0.010 eV above it, in very good agreement with the relatively high-level calculations of Raghavachari and Rohlfing[99] who calculated the difference to be 0.022 eV.

Si_3^- and Si_4^-. Smalley and co-workers have looked at the conventional photodetachment spectra of a

range of silicon (and germanium) clusters, Si_n^- (n = 3−12).[100] In that work, negative ions were selected from the various species present in a molecular beam that contained the products of laser vaporization of a silicon target. The photodetachment of the (mass-selected) negative anions was by the output from an ArF laser. Kinetic energy analysis of the photodetached electrons was achieved by a magnetic bottle-type analyzer[75] (as mentioned above). The spectra obtained were rather broad in general (resolution ~1000 cm^{-1}), but allowed the photodetachment thresholds to be determined. Kitsopoulos *et al.*[101] obtained much higher resolution spectra (~70 cm^{-1}). Clusters were produced in a similar way to the previous study, but photodetachment was now performed by the third and fourth harmonics of a Nd:YAG laser. For the spectrum of Si_3^- (using the 355 nm radiation) two bands were seen, the first was sharp (band B), whereas the second (band X) was broad and demonstrated a progression of nine peaks with a measured spacing of 360 ± 40 cm^{-1}. When 266 nm radiation was used, another weak feature was seen between these bands (band A), having five peaks with a measured spacing of 480 ± 40 cm^{-1}; two other bands to lower electron kinetic energy were seen, the lower feature had two peaks separated by 480 cm^{-1}, and the other showed irregular structure. Interpretation of this spectrum was not performed in any detail owing to the lack of consistency of proposed interpretations with a range of *ab initio* calculations. For Si_4^-, the situation was more consistent; however discussion is left until the discussion of the ZEKE results.

The ZEKE spectrum of the Si_3^- (see Figure 7) complex was recorded by Arnold and Neumark[102] with a resolution of 10−15 cm^{-1}. Only the broad, higher energy feature (band X) gave rise to a ZEKE spectrum. The structure in this spectrum was dominated by a progression with a spacing of 337 cm^{-1}. There were also weaker features seen in the spectrum, and a peak lying 385 cm^{-1} to the red of the origin of the 337 cm^{-1} progression.

In order to discuss the assignment of the spectrum, the electronic structure of the Si_3 molecule needs to be considered. The electronic configuration of the first two states (D_{3h} symmetry) is $(1a_1')^2(1e')^4(2a_1')^2(1a_2'')^2(2e')^2$ giving rise to three electronic states: $^3A_2'$, $^1E'$ and $^1A_1'$. The $^1E'$ state can distort owing to the Jahn−Teller effect and gives rise to two states: a $^1A_1$ state and a $^1B_2$ state, each arising from the splitting of the degeneracy of the e′ orbitals into a_1 and b_2 orbitals, under C_{2v} symmetry. Clearly, under D_{3h} symmetry, the anion has $^2E'$ symmetry and is thus also subject to Jahn−Teller distortion—to a $^2A_1$ state and a $^2B_2$ state; the $^2A_1$ state is the ground state, according to QCISD(T) calculations.[99,103] Large calculated differences in the bond angle between the anion and the neutral state led Arnold and Neumark to consider the assignment of the 337 cm^{-1} vibration to the symmetric bend mode, ν_2, of the $^1A_1$ state. However, calculations suggested that this assignment could not be correct since the calculated vibrational frequency was far too low. Thus, the assignment to the $^3A_2'$ state was favored. QCISD(T) and SCF calculations gave values that were in poor agreement

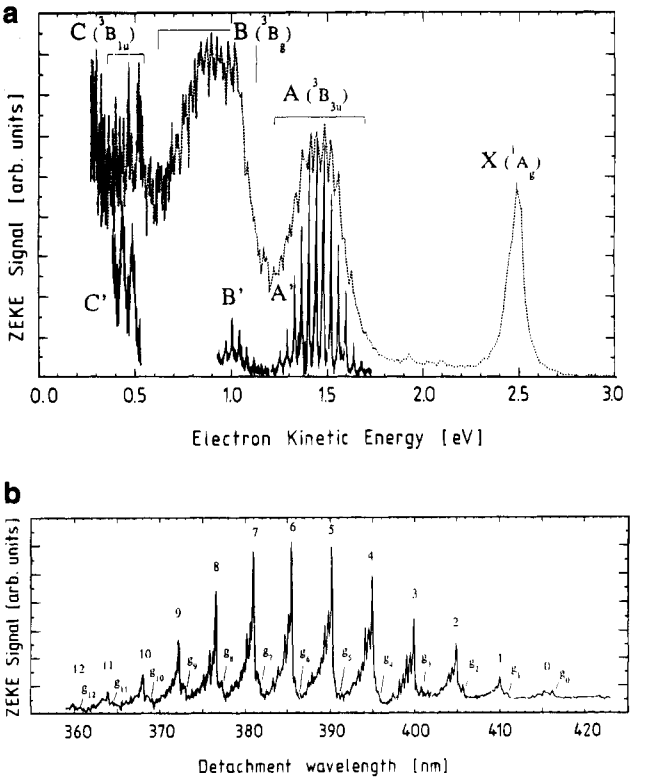

Figure 7. Part a shows the ZEKE spectrum of Si_4^- (solid lines) is superimposed onto the energy scale of the photoelectron spectrum (dotted line). (Taken from ref 105.) Part b shows a finer step scan of the A′ band shown in a to show more detailed structure of that band. (Taken from ref 105.)

with the experimental frequency, whereas density functional calculations[104] were in much better agreement. For these reasons, the assignment of band X was taken to be due to the $^3A_2' \leftarrow {}^2A_1$ photodetachment, with the 337 cm^{-1} progression being assigned to a progression of the ν_2 vibration of the neutral. Some of the weaker features were assigned to components of a ν_2 progression, each component of which was in combination with one quantum of the ν_1 vibration, measured at 501 ± 10 cm^{-1}. Other features in the spectrum were assigned to hot band structure. Simulations were then performed to try and understand the spectrum in more detail. The best agreement was obtained with a treatment including the quadratic Jahn−Teller effect, although there were still inconsistencies between the experimental data and calculations.

As noted above, the conventional photodetachment spectrum of Si_4^- (see Figure 7a, dotted line) showed a large amount of vibrational structure. Assignment of this spectrum was tentative, but recent *ab initio* calculations suggested a consistent assignment, and this is indicated in Figure 7a. The ZEKE spectral scans[105] are shown beneath the conventional photodetachment spectrum (Figure 7a, solid line). Band X did not give rise to any ZEKE intensity; band A gave a rich vibrational structure (marked as A′); only part of band B gave rise to any ZEKE structure (marked as B′); and band C gave rise to the structure labeled as C′. Band A′ is shown enlarged in Figure 7b, as may be seen it shows additional resolved structure on the individual vibrational components (which have a spacing of 312 cm^{-1}). That the intensities of the weak features to either side of the

most intense feature varied with the molecular expansion conditions, indicated that they were due to hot band features arising from vibrational excitation in the anion. The weaker features to the blue of the intense peaks were separated into two progressions of *ca.* 50 and 30 cm^{-1}; the two features to the red had spacings of *ca.* 25 and 53 cm^{-1}. Band A was assignable to the $^3B_{3u} \leftarrow {}^2B_{2g}$ photodetachment by considering the *ab initio* calculation,[103] with regard to energy and to vibrational frequency (the ν_2 mode was calculated to have a harmonic frequency of 306 cm^{-1} for the $^3B_{3u}$ state), and expectations based upon the changes in geometry between the neutral and anionic states. Locating the origin of this progression proved difficult owing to low intensity at the onset of the band. Franck–Condon simulations together with the *ab initio* data led to the conclusion that band 0 marked in Figure 7b was indeed the origin of the band. The weak features were assigned by further FC calculations and by comparison with the *ab initio* calculations.

Band B′ again showed a main progression flanked by weaker features, the main progression had a frequency of 300 ± 6 cm^{-1}. The assignment of this band was based upon the fact that the only state calculated[103] to be in this energy region, which also could be formed by *s*-wave photodetachment from the anionic state, was the $^1B_{3u}$ state. The irregular vibrational structure of the weaker features was postulated as being due to vibronic coupling between the electronic states that were calculated to lie within the range of band B in Figure 7a, but that could not be formed by photodetachment of an *s* wave.

Band C′ was rather broad owing to the use of only a partial discrimination against higher kinetic energy electrons (with a view to increasing the intensity of the rather weak feature). The structure consisted of a progression of *ca.* 430 cm^{-1}. The assignment to the $^3B_{1u} \leftarrow {}^2B_{2g}$ photodetachment transition[103] was deemed the most likely.

iv. Transition States

During the hydrogen-exchange reaction A + HB → AH + B, there is a transition state formed that has the hydrogen partway between the A and B moieties.[106] These complexes have been probed over the last five years or so by Neumark and coworkers[107–109] by looking at photodetachment from the AHB^- complex. The complexes $ClHCl^-$, $BrHBr^-$, and IHI^- have been studied by conventional photodetachment spectroscopy, as has the related complex, H_2F^-.[110] *Ab initio* calculations have been performed on these species, with the work up until the beginning of 1993 having been summarized by Klepeis *et al.*[111] in their comprehensive *ab initio* study of the $FHCl^-$ complex. Only one experimental study (to date) has looked at one of these complexes using ZEKE spectroscopy: this is the study of Waller *et al.*[112] on IHI^-. The latter complex has attracted a significant amount of attention recently with an *ab initio* study by Schatz *et al.*[113] being the most recent one at the time this review was written. Only the IHI^- complex will be considered here.

In the conventional photodetachment study, Weaver *et al.*[108] looked at IHI^- and IDI^- stimulated by a number of facts. One was that a matrix isolation study of IHI^- had been reported by Ellison and Ault,[114] which had indicated that IHI^- was linear and centrosymmetric as was expected for the transition state of the I + HI → IH + I reaction. Also, calculations had predicted that bound states of the IHI complex existed.[115] Thus, it was anticipated that the vertical (most intense) region of the photodetachment spectrum of IHI^- would give direct information on the IHI transition state. In the experiment, HI was expanded in argon through a pulsed valve and it was then crossed by a 1 keV electron beam. The resulting mixture of ions and neutrals then cooled in the subsequent expansion. The IHI^- species were mass selected and the anions then underwent photodetachment by the fourth harmonic of a Nd:YAG laser. The resulting electrons were kinetic-energy analyzed: spectral resolution was *ca.* 8 meV. A series of three peaks was seen in the spectrum and these were assigned to a progression of double quanta of the asymmetric stretch, ν_3. Spectral simulation indicated that there should also be symmetric stretch quanta associated with each of the transitions in the asymmetric mode, but that these were not resolved in this experiment. Owing to the poor spectral resolution, it was not possible to be certain that any of the states of IHI, accessed in the photodetachment, were bound; and indeed thermodynamics seemed to suggest that all the observed levels were quasi-bound. The most likely candidate for a bound state was a narrow peak observed in the IDI^- spectrum.

The ZEKE spectrum[112] was more definitive, however, with 30 cm^{-1} wide peaks being observed. In this study, the IHI^- ions were produced and selected as in the previous experiment, but on this occasion they underwent photodetachment by the output of a tunable dye laser: the experimental resolution was between 1 and 2 meV. In this higher resolution experiment, the expected symmetric stretch vibration of the IHI complex were resolved for the $\nu_3 = 0$, 2, and 4 transitions. They exhibited significantly different widths which were taken to be indicative of the different lifetimes of the levels in the neutral complex's states. For example, in the $\nu_3 = 4$ level, two components of a symmetric stretch vibrational progression were observed (93 ± 5 cm^{-1}) and were assigned to $\nu_1 = 0$ and 1; these demonstrated spectral widths that indicated lifetimes of 180 and 120 fs, respectively. Hot bands in this latter feature showed vibrational structure that basically agreed with the matrix isolation data.[114] For the $\nu_3 = 2$ feature, the peaks were somewhat broader (100 cm^{-1}), and also had spacings of *ca.* 100 cm^{-1}. In contrast, the $\nu_3 = 0$ level had shown a series of peaks whose spacing varied from 160 to 200 cm^{-1} to higher laser energy. However, this was to be expected as calculations had suggested that photodetachment to this level was expected only to access direct scattering wave functions rather than quasi-bound levels. Interestingly, comparison between the ZEKE experiment and the calculations showed that only high rotational energy levels of the IHI complex had significant intensity near to threshold. Also of note is that both a three-dimensional adiabatic model,[116] and the recent *ab initio* calculation[113] indicate a sharp feature at thresh-

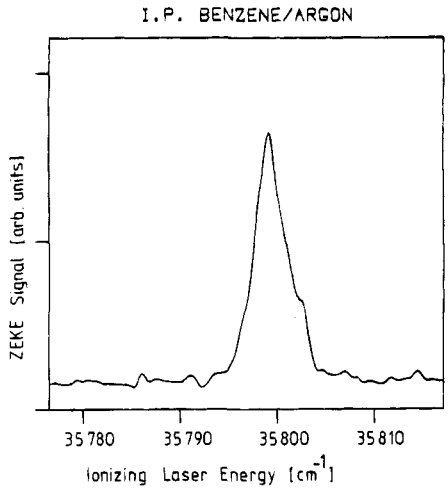

Figure 8. ZEKE spectrum of benzene–Ar over the ionization energy region. (Taken from ref 117.)

old that does not appear in the ZEKE spectrum.

c. van der Waals Complexes Containing Organic Molecules

i. Miscellaneous

The first such ZEKE study was that on the benzene–Ar complex by Chewter *et al.*[117] in 1987. Although only a single band was observed (see Figure 8) it allowed the AIE to be determined as 74383 ± 2 cm^{-1}, giving a lowering in the AIE of 172 cm^{-1} with respect to the value of the AIE of benzene[118] which was current at that time (see Table 3). Similarly, the AIE and the respective complexation shift of *p*-difluorobenzene–Ar were obtained[16,119] and are given in Table 3.

Cockett *et al.*[120] studied the *p*-dimethoxybenzene–Ar_n (n = 0, 1, and 2) complexes. They used a two-step 1 + 1′ ionization scheme for the recording of the ZEKE spectra. The first stage in the experiment was to ascertain the positions of the origins of the *p*-dimethoxybenzene–Ar_n (*p*-DMOB–Ar_n) $S_1 \leftarrow S_0$ origins, via a 1 + 1 REMPI experiment. A complication arises in that there are two rotational isomers of *p*-DMOB corresponding to the OCH_3 groups being *cis* and *trans* to each other. The n = 1 and n = 2 origins were found to be red shifted from the *cis* n = 0 origin (at 33 858 cm^{-1}) by 49 and 78 cm^{-1} and from the *trans* n = 0 origin (at 33 637 cm^{-1}) by 48 and 76 cm^{-1}, respectively. Assignment of the $S_1 \leftarrow S_0$ features had been made previously by Ito and coworkers.[121] By appropriate choice of the excitation wavelength it was possible to *spectroscopically select* each of the *p*-DMOB–Ar_n complexes (and their *cis* and *trans* isomers) in turn, and obtain a ZEKE spectrum of each. The ZEKE spectrum of the noncomplexed *cis* and *trans* isomers of *p*-DMOB each showed just one feature in addition to the AIE peak in the 0–100 cm^{-1} range, this was a low-energy feature at 75 and 69 cm^{-1} to the blue of the respective origins; these features were tentatively assigned to a methoxy torsional mode. For each of the isomers with n = 1, other low-energy features were seen that were assigned to the intermolecular stretch and intermolecular bending modes. The situation was more complicated for the isomers of the n = 2 complexes (where the argon atoms are on either side of the benzene ring, in a "sandwich" conformation); however, a consistent assignment of all features was achieved in terms of the various intermolecular modes. One interesting point was that although the ZEKE spectra that were due to *cis* and *trans* isomers were quite similar, those due to the n = 2 isomers were quite different. The ionization energies and their shifts relative to the parent molecule are collected in Table 3.

Dyke *et al.*[122] studied the ZEKE spectra of the two compounds styrene and phenylacetylene and their Ar complexes. ZEKE spectra of the parent molecules were recorded via different vibrational levels of the S_1 state. The ZEKE spectra of the corresponding Ar complexes (recorded only via the vibrationless S_1 origins) were rather broad, but progressions of a vibration of 15 cm^{-1} could easily be resolved; this vibration was assigned as an a′ intermolecular bending vibration in each case, by comparison with known

Table 3. Adiabatic Ionization Energies (AIE) and Respective Complexation Shifts (ΔAIE) of Some Organic Molecules and Clusters Studied with ZEKE Spectroscopy

species	AIE	ΔAIE	ref(s)
van der Waals-Bonded Species			
benzene	74555		118
benzene–Ar	74383	−172	117
p-difluorobenzene	73870		16
p-difluorobenzene–Ar	73637	−233	16,119
aniline	62281		125
aniline–Ar	62168	−113	125
aniline–Ar_2	62061	−220	125
aniline–CH_4	62112	−169	125,126
p-dimethoxybenzene (cis)	60774		120
p-dimethoxybenzene–Ar (cis)	60687	−87	120
p-dimethoxybenzene–Ar_2 (cis)	60509	−265	120
p-dimethoxybenzene (trans)	60563		120
p-dimethoxybenzene–Ar (trans)	60479	−84	120
p-dimethoxybenzene–Ar_2 (trans)	60295	−268	120
styrene	68267		122
styrene–Ar	68151	−116	122
phenylacetylene	71175		122
phenylacetylene–Ar	71027	−148	122
toluene	71199		123
toluene–Ar	71033	−166	123
toluene–Ar_2	70871	−328	123
phenylsilane	73680		124
phenylsilane–Ar	73517	−163	124
phenylsilane–Ar_2	73359	−321	124
anthracene	59872		132
anthracene–Ar			132
isomer I (1:0)	59807	−65	
isomer II (1:0)	59825	−47	
anthracene–Ar_2			132
isomer I (1:1)	59757	−115	
isomer II (2:0)	59774	−98	
anthracene–Ar_3			132
isomer I (2:1)	59695	−177	
anthracene–Ar_4			132
isomer I (3:1)	59660	−212	
isomer II (2:2)	59606	−266	
anthracene–Ar_5			132
isomer I (3:2)	59565	−307	
Hydrogen-Bonded Species			
phenol	68628		165
phenol–water	64027	−4601	135
phenol–methanol	63207	−5421	136
phenol–ethanol	62901	−5727	137
phenol–dimethyl ether	62604	−6024	139
phenol dimer	63649	−4980	138

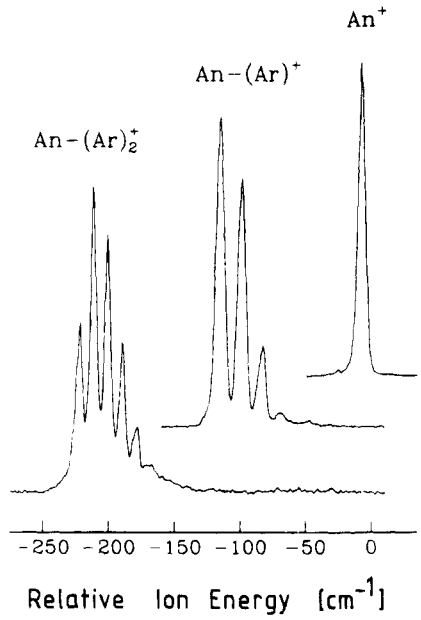

Figure 9. ZEKE spectra of aniline (An) and An–Ar_n complexes (n = 1 and 2) via the respective vibrationless S_1 origins. (Taken from ref 125.)

values of the neutral complex in the S_0 and S_1 states. Values for the ionization energies and shifts relative to the respective monomers are given in Table 3.

Lu *et al.* in their studies of the internal rotation in toluene[123] and phenylsilane,[124] also obtained the AIEs for the corresponding Ar and Ar_2 complexes (although no spectra for the complexes were shown in the papers). The values of the AIEs and their shifts relative to the parent molecules are given in Table 3.

ii. Aniline–Ar, –Ar_2, and –CH_4

By far the most detailed ZEKE spectroscopic study on van der Waals complexes has come from Knee and co-workers using nanosecond and picosecond lasers.[125,126] The study was on the three complexes: aniline–Ar, aniline–Ar_2, and aniline–CH_4. Although another study on the aniline–Ar_n (n = 0, 1, and 2) complexes[127] and one on aniline alone[128] have appeared, only the studies by Knee and co-workers[125,126] will be considered explicitly, here.

The ZEKE spectra of aniline (An) were recorded via different vibrational levels of the S_1 state and an accurate value of the ionization energy was obtained which was in good agreement with the other two ZEKE studies (although there is a 10 cm^{-1} spread in the values obtained). There was a small amount of vibrational excitation in the REMPI spectra corresponding to the An–Ar_n (n = 1, 2) van der Waals species, and these had been previously assigned to intermolecular modes, excited in the $S_1 \leftarrow S_0$ transition by Bieske *et al.*[129] By choosing each of the vibrationless S_1 origins for the particular species in turn, ZEKE spectra for each of them could be obtained; these are shown in Figure 9. The progressions assignable to An–Ar and An–Ar_2 were almost perfectly harmonic (to within 1 cm^{-1}) and had frequencies of 15 and 11 cm^{-1}, respectively. Note, that only one mode is excited in each case and that the assignment is to the symmetric intermolecular bend in the ion (these are the symmetric bends along the C_{2v} axis, denoted b_{xs} in the case of An–Ar_2; in the case of An–Ar, the bend is denoted b_x). For An–Ar, different intermolecular modes were excited in the S_1 state, prior to ionization—in particular, the b_{x0}^1 and the s_{z0}^1 transitions were used (s_z is the intermolecular stretch)—and these ZEKE spectra showed a different excitation, and in fact the latter excitation allowed the intermolecular stretch in the ion to be determined as 66 cm^{-1}.

By exciting through aniline-localized vibrational modes and using a variable delay between the exciting and ionizing dye lasers, it was possible to follow the phenomenon of intermolecular vibrational redistribution (IVR) in the An–Ar complex. One example of this is shown in Figure 10a where the $\bar{I}_0^2$ vibration has been excited. (The I implies the inversion vibration of the NH_2 group, and the bar indicates that this vibration is located on the complex; for vibrations that are associated with the An monomer, no bar is used.) As the delay time is increased, the spectra indicate that the complex is dissociating in the S_1 state and that the $16a_1^1$ transition of the resulting aniline monomer fragment is seen in the ZEKE spectrum. What is occurring here is that the energy of the $\bar{I}$ vibration (present in the S_1 state) causes dissociation of the complex via IVR into the manifold of the intermolecular vibrations. One dissociation channel leaves the monomer with the ν_{16} vibration excited in the S_1 state, as can be seen in the ZEKE spectrum (see Figure 10a) with the indicated $16a_1^1$ transition. This is a very powerful tool for looking at vibrational redistribution and also vibrational predissociation in the intermediate state, and is complementary to dispersed fluorescence probing. (See for example the work on An–Ar by Nimlos *et al.*[130])

A picosecond study of the An–CH_4 complex was reported very recently[126]—various vibrational levels of the S_1 state[131] were used as intermediate resonances, in order to investigate how the vibrational energy is redistributed. One nice example was that of the $\bar{6}a_0^1$ excitation, the result for which is shown in Figure 10b. A much shorter time scale for the vibrational redistribution, compared to that of the An–Ar complex, is evident. The clearly-resolved vibrational structure, which is due to the intermolecular modes of the cationic complex, may be seen at 0 ps delay, at 400 ps some broadening is evident, and then at 1200 ps, all structure is lost except for the appearance of a band at a position corresponding to the An moiety itself, *i.e.* the complex has dissociated owing to the IVR in the S_1 state. The time for this distribution was measured by sitting on a complex ZEKE peak and measuring the decay of this feature as a function of time; a value of 350 ps was obtained for the 1/e lifetime.

In summary, the time-resolved ZEKE studies of Knee and co-workers have shown that the ZEKE technique is a very powerful tool of monitoring the dynamics in the intermediate state of these species (in these cases IVR and dissociation).

iii. Anthracene–Ar_n (n = 0–5)

Cockett and Kimura[132] have very recently reported their ZEKE study of the anthracene–Ar_n (Ant–Ar_n)

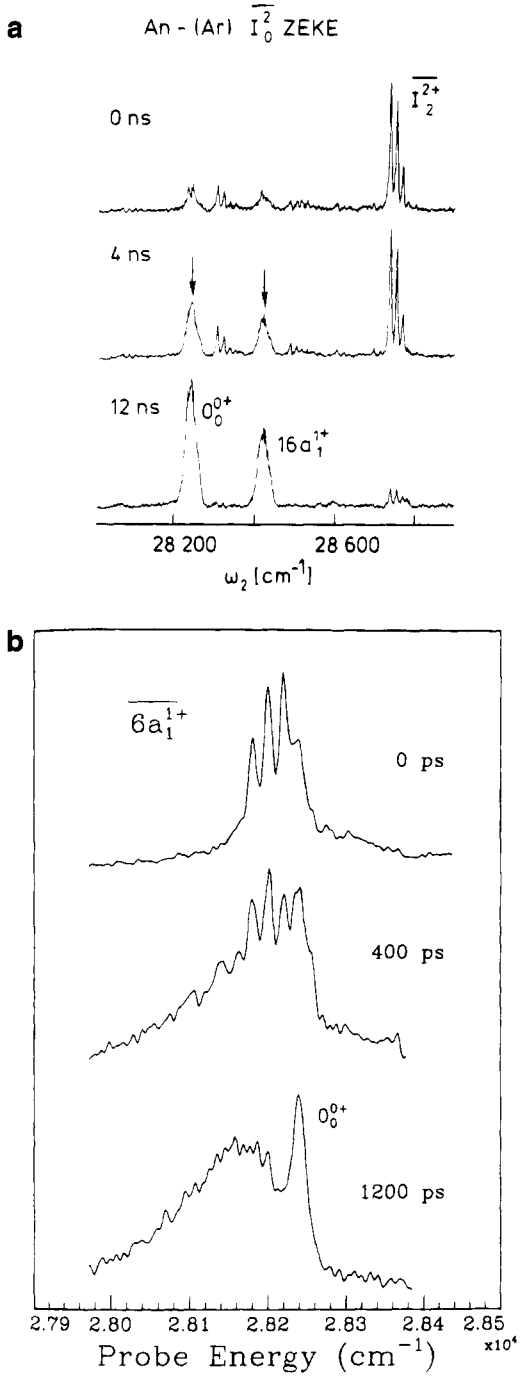

Figure 10. ZEKE spectra of aniline (An) complexes to monitor the dynamics in the S_1 state (dissociation and IVR). (a) ZEKE spectrum of An–Ar via the $S_1\bar{I}_0^2$ level (762 cm^{-1}; *i.e. ca.* 300 cm^{-1} above the dissociation energy of the S_1 state) of the complex as a function of the delay time between pump and probe laser. The features indicated by arrows are product states of the aniline monomer which grow with increasing probe delay time. (Taken from ref 125.) (b) ZEKE spectrum of An–CH_4 via the $S_1\ \bar{6}_0^1$ level of the complex as a function of the delay time between pump and probe laser. The broad structure in the lower trace is due to IVR to the intermolecular van der Waals modes. The sharper peak at late time is the vibrationless aniline dissociation product. (Taken from ref 126.)

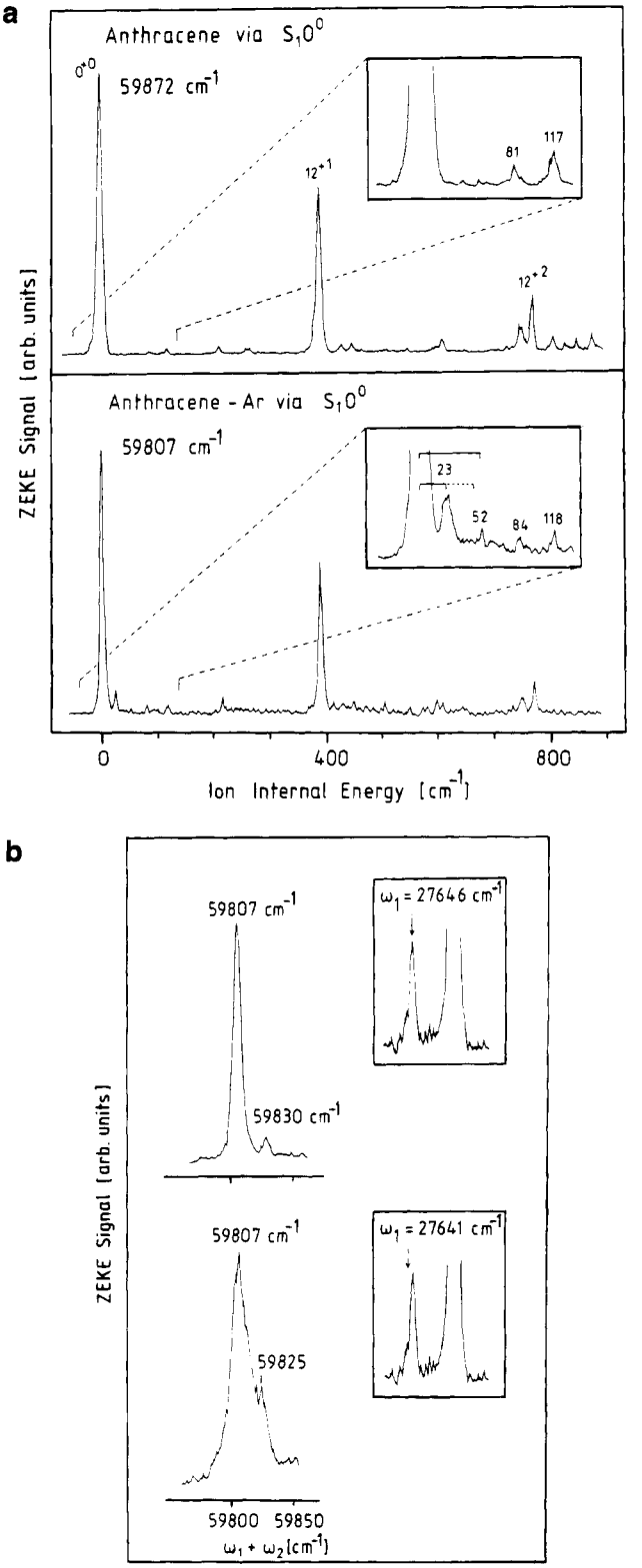

Figure 11. (a) ZEKE spectra of anthracene (top) and the most abundant anthracene–Ar isomer (bottom) recorded via their respective vibrationless S_1 origins. The low ion internal energy region of each spectrum is given in the insets of the figure. (Taken from ref 132.) (b) ZEKE spectra of the more abundant anthracene–Ar isomer (top) and the less abundant anthracene–Ar isomer (bottom) recorded via their respective vibrationless S_1 origins. An indication of the respective exciting laser energy is given in the insets of the figure. (Taken from ref 132.)

complexes. These complexes are of interest since for Ant there are a number of different binding sites; also as the number of Ar atoms increases, then the possibilities for isomerization increases. Studies that have looked at this isomerization for the larger organic polycyclic compounds have been noted in ref 132. The ZEKE spectra obtained by Cockett and

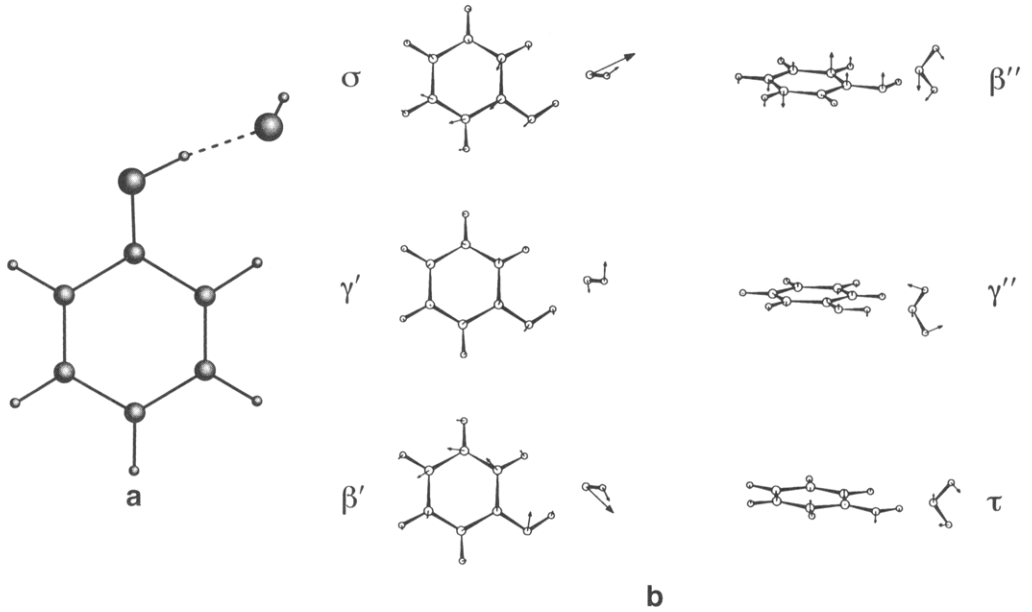

Figure 12. Part a is a sketch of the structure of the ionic 1:1 phenol−water complex (C_s symmetry, the phenyl plane is the symmetry plane). (Geometry taken from ref 158.) Part b shows the six intermolecular normal modes of the phenol−water cation radical: σ is the stretch, τ is the torsion, β' and β'' are the in-plane and out-of-plane bends, while γ' and γ'' are the in-plane and out-of-plane wags. (σ, γ', and β' have a′ symmetry; β'', γ'', and τ have a″ symmetry.) (Taken from ref 158.)

Kimura for Ant and Ant−Ar are shown in Figure 11. The AIE for Ant was determined as 59872 ± 5 cm^{-1}, while that for the Ant−Ar complex was determined as 59807 ± 5 cm^{-1}. The low-frequency modes (see insert of Figure 11a, top) in the Ant ZEKE spectrum were not assigned definitively, but it was suggested that they were due to out-of-plane bending modes. In the Ant−Ar ZEKE spectrum (Figure 11a, bottom), low-frequency features at 23 and 52 cm^{-1} were also seen and these were assigned to the intermolecular modes excited upon ionization. The specific assignment was to two quanta of the bending mode in the x direction (23 cm^{-1}) and two in the y direction (52 cm^{-1}); the latter was also suggested as being possibly due to one quantum of the intermolecular stretch. It was noted that a weak shoulder appeared on the red side of the origin peak in the REMPI spectrum under certain jet conditions, and it was thought that this could be due to another isomer of Ant−Ar, with the Ar atom on one of the end rings of the Ant molecule, rather than on the central ring, as in the more stable isomer. To test this hypothesis, the laser was tuned to the red of the center of the peak, and indeed the ZEKE spectrum did show a shoulder appearing to the blue of the more stable isomer (see Figure 11b), corroborating the second isomer hypothesis. For Ant−Ar_2, again evidence for two isomers was obtained (assuming one isomer with the two Ar atoms over the central rings, on opposite sides; the other with the Ar atoms on different terminal rings, on the same side). Low-frequency intermolecular features were seen in the ZEKE spectrum, and so attempts at assigning them were made by recourse to symmetry arguments; however, the assignment was rather speculative.

For Ant−Ar_3, the most stable isomer has two argon atoms on terminal rings on the same side, with the third Ar atom on the central ring, on the opposite side. The assignment of the vibrational structure seen in this spectrum was not possible although an intermolecular bend was offered. Lastly, for Ant−Ar_4 and Ant−Ar_5 no clear vibrational structure was seen. All ionization energies and shifts relative to the respective parent molecule are given in Table 3.

d. Hydrogen-Bonded Complexes

The study of hydrogen-bonded species using ZEKE spectroscopy has mainly taken place in Munich, over the last three years. To date, five different hydrogen-bonded species have been studied, all involving phenol as the proton-donating moiety. Specifically, these complexes are phenol−water[133−135] (Ph−H_2O), phenol−methanol[136] (Ph−MeOH), phenol−ethanol[137] (Ph−EtOH), phenol dimer[138] (Ph_2), and phenol−dimethyl ether[139] (Ph−DME). In addition to these intermolecular complexes, the intramolecularly hydrogen-bonded complexes tropolone[140] and 9-hydroxyphenalenone[141] have been studied by Kimura and co-workers. In reviewing this work, it has been decided to collect the data on the series of complexes Ph−H_2O, Ph−MeOH and Ph−EtOH together; then the Ph_2 complex will be reviewed, where ring−ring interactions are possible; and penultimately the Ph−DME complex will be considered. Finally, the two intramolecularly bonded complexes will be described, where electronic and geometric factors have been considered in the bonding.[140,141]

i. Phenol–Water, Phenol–Methanol, and Phenol–Ethanol

Phenol−Water. Initially, the experimental data on the phenol−water complex will be summarized. This complex, and indeed the series of complexes phenol−$(water)_n$ (n = 1−4), has received much attention over the last 10−15 years. Experimental techniques that have been employed include REMPI spectroscopy,[135,142−148] laser-induced fluorescence (LIF),[2,142,149,150] and phosphorescence[151] spectroscopy,

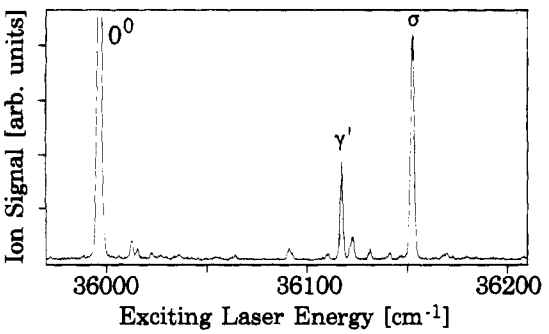

Figure 13. Two-photon, two-color (1 + 1′) REMPI spectrum of the phenol–water complex (ionizing laser wavelength was 350 nm). The intermolecular stretch and in-plane wag vibrations are indicated by σ and γ', respectively. The S_1 origin is out of scale and by a factor of *ca.* 2–3 higher than the stretch band. The weak features in the region up to 50 cm^{-1} above the S_1 origin are due to fragmentation of phenol–water–Ar complexes. (Taken from ref 148.)

spectral hole burning,[152] ion-dip experiments,[146,153] ionization-loss stimulated Raman spectroscopy (IL-SRS),[154] and stimulated emission ion dip spectroscopy (SEID).[150,155] A number of *ab initio* studies on the neutral ground electronic state have also been published,[147,156-158] all agreeing that the water is bonded symmetric with respect to reflection in the plane of the phenol ring (similar to the structure of the ionic complex which is shown in Figure 12a): the symmetry is thus C_s. The experimental studies on the 1:1 complex have concentrated on the first excited singlet state S_1 (formed by a $\pi^* \leftarrow \pi$ excitation on the phenol ring) in the main, although some information is available on the ground state (S_0). The 1 + 1′ REMPI spectrum of the Ph–H_2O complex shows only a meager amount of structure (see Figure 13). The transition into the vibrationless state is the most intense transition, suggesting that the geometries of the S_1 and S_0 states are fairly similar—at least along the hydrogen-bonding coordinates; two other intermolecular vibrations appear, the reasonably strong stretch vibration (σ) at 156 cm^{-1} and the weak in-plane wag vibration (γ') at 121 cm^{-1}. The assignments of these bands have been refined over the years and a brief résumé of the stages in this refinement is warranted.

First of all, the energy of the $S_1 \leftarrow S_0$ transition has been established[135] as being at 35996.2 ± 1 cm^{-1}, which represents a shift of 352.5 cm^{-1} to the red of the corresponding transition of phenol (measured by Levy and co-workers[159] to be at 36348.7 cm^{-1}). Initially, Abe *et al.*[142] assigned the 121 cm^{-1} vibration (in a fluorescence excitation experiment) to the intermolecular stretch, while the 156 cm^{-1} band was hypothesized as either being due to another isomer of the 1:1 complex, or as being due to a higher complex. However, in a subsequent paper[149] this assignment was changed with the 156 cm^{-1} vibration being assigned to the intermolecular stretch and the 121 cm^{-1} feature to a bending mode, although the reasoning as to why was not presented. Lipert and Colson[145] agreed with the latter assignment in their study which employed the one-color REMPI technique, but with the 121 cm^{-1} band being reassigned to a wagging mode on the basis of experiments on deuterated samples. More recently, Leutwyler and co-workers[147] have obtained a very high quality 1 + 1′ REMPI spectra of the phenol–water complex. Comparison of the spectra with *ab initio* calculations confirmed the previous spectral assignment given by Lipert and Colson.[145] In addition, more bands were seen in the low-energy region of the REMPI spectrum and assignments of these features were proffered.

Vibrational information on the ground electronic state has been obtained by the techniques of dispersed fluorescence spectroscopy, ion-dip spectroscopy, and the related SEID spectroscopy. The dispersed fluorescence experiments[147] have determined the ground state intermolecular stretch frequency to be 155 cm^{-1}, *i.e.* very similar to that in the S_1 state, indicating that the bonding of the S_1 and S_0 states are very similar. The in-plane wag, γ', was determined to be 146 cm^{-1}.

In contrast to the neutral states of the 1:1 phenol–water complex, information about the low-frequency intermolecular vibrations of the *ionic* complex was rather sparse (before the ZEKE studies). A conventional (one-color, two-photon) time-of-flight photoelectron spectrum (REMPI-PES)[160] via the vibrationless S_1 state does not show resolved structure due to intermolecular modes: the vibrations of most interest. Two-color photoionization efficiency (REMPI-PIE)[144] measurements via the vibrationless S_1 origin and the S_1 level with one quantum of the intermolecular stretch excited showed the presence of at least one intermolecular vibration which was observed as a progression of steps in the ion yield spectra. This vibration of 242 cm^{-1} was assigned to the intermolecular stretching mode of the ionic complex. However, no further (out of a possible six) intermolecular modes have been obtained. Finally, Mikami *et al.*[161] used the technique of trapped ion photodissociation spectroscopy to confirm that proton transfer does not take place in the cationic complex.

The first ZEKE spectroscopic study on the Ph–H_2O complex was by Reiser *et al.*[133] in 1991. The reported spectrum was obtained via a two-step process: first the vibrationless S_1 state was populated with one dye laser and then the other dye laser was scanned toward the ionization threshold and the long-lived Rydberg states were ionized by the electric extraction pulse. The spectrum showed clearly-resolved vibrational structure that was evidently attributable to the intermolecular modes of the complex. (The complex itself was formed by heating phenol and water in a stainless steel oven and expanding the mixture, diluted in argon, through a nozzle, thus forming a supersonic expansion that cooled the internal energy of the complex considerably.) The assignment of the structure in the spectrum to particular intermolecular modes was not straightforward, and indeed the interpretation presented in that paper, and a subsequent one[134] was revised later.[135] The main conclusion, namely that the spectrum was dominated by a progression in the intermolecular stretch with a frequency of 240 cm^{-1}, remained unchanged in the later interpretation (*vide infra*). It is noted that a preliminary report of the phenol–water ZEKE spectrum was also made by Kimura and co-workers,[162] where the intermolecular stretch progression was also seen.

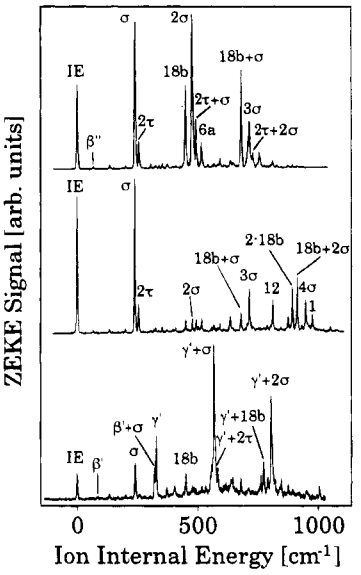

Figure 14. ZEKE spectra of the 1:1 phenol–water complex, [Ph–H_2O]-h_3, via different intermediate S_1 levels: S_1 0^0 (top), S_1 σ^1 (middle), and S_1 γ'^1 (bottom). (Taken from ref 135.)

Very recently, a more complete ZEKE spectroscopic study[135] of the 1:1 phenol–water complex has been presented including the study of the 3-fold deuterated complex (where the two water hydrogens and the phenolic hydrogen have been substituted by a deuterium atom); these are denoted [Ph–H_2O]–h_3 and [Ph–H_2O]-d_3, respectively. Considering the [Ph–H_2O]-h_3 complex, the ZEKE spectra were obtained by exciting through three intermediate vibronic states, the S_1 0^0, the S_1 σ^1, and the S_1 γ'^1 states; the resulting spectra are shown in Figure 14. The first point that must be addressed is the value of the AIE; this had been previously determined by Fuke *et al.*[160] as 8.09 eV (~65250 cm^{-1}), from a REMPI-PES experiment where the kinetic energy electrons associated with the ionization had been analyzed. In the REMPI-PIE experiment, where the ion yield as a function of laser frequency had been recorded, Lipert and Colson[163] obtained a much more accurate value for the AIE of 64035 ± 10 cm^{-1}. This value was obtained by measuring the PIE onset as a function of extraction voltage and then extrapolating to zero field [by using the well known $\delta = c\cdot\sqrt{F}$ relationship—where δ is the lowering in ionization energy in cm^{-1}, by the electric field F in volts per centimeter (see also Figure 1b)]. Interestingly, the proportionality constant c was not equal to 6.1 as expected from a classical picture,[164] but was equal to 4.5. From the ZEKE experiment, the AIE was taken as the sum of the laser energies that corresponded to the first vibrational band in the ZEKE spectrum; this gave a value of 64024 ± 4 cm^{-1}. A lowering in the ionization energy of 3 cm^{-1} was estimated due to the extraction field of 0.7 V/cm, and considering the fact that many of the lower Rydberg states will have predissociated before the application of the electric field. This shift is also in agreement by comparison with an accurate determination of the ionization energy of NO[20] under the same extraction conditions. (This shift used was then for all hydrogen-bonded phenol–X complexes as the extraction conditions have not been changed.) This then leads to an

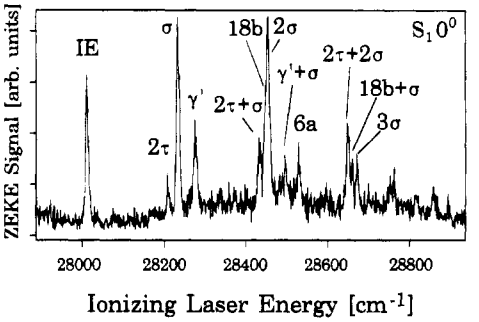

Figure 15. ZEKE spectrum of the 3-fold deuterated 1:1 phenol–water complex, [Ph–H_2O]-d_3 (*i.e.* PhOD–D_2O), via the S_1 0^0 level. (Taken from ref 135.)

(field-free) AIE of 64027 ± 4 cm^{-1}. This value was, within experimental error, the same from all three intermediate states. For the deuterated sample, a field-corrected AIE of 64020 ± 4 cm^{-1} was obtained. The AIE of the [Ph–H_2O]-h_3 complex is lower by 4601 ± 8 cm^{-1} compared to the ionization energy of the isolated phenol molecule[165] (68626 ± 4 cm^{-1}). The AIE values and the lowering in the ionization energy upon complexation are summarized in Table 3.

From the recent work, five out of a possible six intermolecular vibrations (shown in Figure 12b) were extracted. As noted above, the most obvious feature was the progression of the intermolecular stretch (see Figure 14); however, the components were also seen in combination with other intermolecular modes. This long progression (consisting of five quanta) of the intermolecular stretch is indicative of the expected large change in the hydrogen-bond length upon ionization. It is also notable that this progression is so strong—it is also seen in the photoionization efficiency measurements,[144] and in fact a bond decrease of 0.018 Å was estimated in that work from a one-dimensional FCF calculation. The progression itself was found to be quite anharmonic—a general finding from the ZEKE spectra of the different hydrogen-bonded complexes (*vide infra*). The increase of frequency of the intermolecular stretch of the cation (240 cm^{-1}) over that in the S_1 state (157 cm^{-1})[135] and the S_0 state (155 cm^{-1})[147] illustrates the large increase in binding energy upon ionization. The other intermolecular vibrations that were observed are (see Figure 12b for illustration of the intermolecular normal modes of the ionic complex) the out-of-plane bend (β'') at 67 cm^{-1}, the in-plane bend (β') at 84 cm^{-1}, and the in-plane wag (γ') at 328 cm^{-1}. For the torsion, only the first overtone (2τ) was observed at 257 cm^{-1}; the out-of-plane wag (γ'') has not yet been identified. Hence, five intermolecular modes are believed to have been identified. Various arguments were used for the specific assignment of these modes, including the magnitude of vibrational frequency shifts on deuteration (a spectrum of the [Ph–H_2O]-d_3 complex via the vibrationless S_1 origin is shown in Figure 15), comparison with the *ab initio* calculations[158] that were carried out concurrently and observation of the variations in intensity as the intermolecular S_1 vibronic level was changed. One good example for the latter point may be clearly seen in Figure 14: in the ZEKE spectrum via the intermolecular S_1 γ'^1 level (bottom) the ionic intermolecular in-plane wag (γ') is strongly enhanced (and also the

Table 4. Comparison of Experimental and Theoretical (Harmonic) Frequencies (in cm^{-1}) of the Intermolecular Vibrations of the Phenol–Water Cation[a]

vibration	experiment[b]	*ab initio*[c]
out-of-plane bend	67/64(?)	87/82
β''	(1.05)	(1.06)
in-plane bend	84/–	124/117
β'	(–)	(1.06)
torsion	~130/~100[d]	202/163
τ	(~1.3)	(1.24)
stretch	240/221	275/259
σ	(1.09)	(1.06)
in-plane wag	328/264	358/259[e]
γ'	(1.24)	(1.38)
out-of-plane wag	–/–	451/330
γ''	(–)	(1.37)

[a] Presented are the values for the [Ph–H_2O]–h_3 and [Ph–H_2O]–d_3 complex as well as the corresponding ratio (in brackets). [b] From ref 135. Only the favored assignment is presented. For alternatives see ref 135. [c] From ref 158; (ROHF/3-21G*(O)). [d] Estimated fundamental frequencies, since only the overtones are observed at 257 and 197 cm^{-1}, respectively. [e] One-dimensional anharmonic approach.

intermolecular stretch progression starting on that particular vibrational origin) compared to the other two ZEKE spectra via the S_1 σ^1 (middle) and S_1 origin level (top). (*If the geometry of the S_1 state and that of the ion are similar along a particular normal coordinate*, and if this vibrational mode will be the most intense mode in the ZEKE spectrum.) The experimental and *ab initio*[158] frequencies of the intermolecular vibrations of the ionic [Ph–H_2O]-h_3 and [Ph–H_2O]-d_3 complexes are summarized in Table 4. (Only the favored assignment is presented here; alternatives are discussed in detail in ref 135.) One point of interest is that the intramolecular ν_{18b} vibration was found to couple strongly with the intermolecular stretch—this point was used to explain why this vibration appeared so prominently in the ZEKE spectrum of this complex, while it was seen only weakly in the ZEKE spectrum of the isolated phenol molecule. The latter coupling was identified from normal mode pictures obtained via the *ab initio* calculations[158] of the vibrations.

Phenol–Methanol. The Ph–MeOH complex was studied in a similar way to that of the Ph–H_2O complex. A mixture of phenol and methanol was heated in a stainless steel oven and the resulting vapor was expanded with Ar through a nozzle into vacuum. The 1 + 1′ REMPI spectrum was difficult to interpret owing to the proximity of a number of vibrations. Both LIF and REMPI spectra of the S_1 state have been reported by Ito and co-workers,[142,149,166] but only sparse interpretation was given, namely that the low-frequency region contained a progression of a vibration of 28 cm^{-1} assigned to an intermolecular bend, and a higher frequency vibration of 175 cm^{-1} assigned to the intermolecular stretch; however, there was clearly more structure in these spectra. Indeed, similar structure was observed in the LIF and REMPI spectra of the *p*-cresol–methanol complex[167] (*p*-cresol = *p*-methylphenol), where some further attempts at interpretation were made. In ref 136, again some further attempts were made at assigning the low-energy region of the Ph–MeOH spectrum. Although some success was achieved, it proved difficult to reach a definitive assignment of the region in terms of six intermolecular modes, although a consistent assignment was reached. Vibrational levels in the S_1 state were used as intermediate states on the way to ionization. The ZEKE spectrum obtained by exciting via the S_1 vibrationless level was particularly striking (see Figure 16) with progressions of *ca.* 10 quanta of a low-frequency vibrational mode of 34 cm^{-1}, denoted η_1,[168] appearing in combination with components of an anharmonic progression of the intermolecular stretch of 278 cm^{-1}. This pattern obviously suggests a rather substantial change of geometry upon ionization. The adiabatic ionization energy was derived as 63207 ± 4 cm^{-1} (field-free value) which represented an increase of bonding over that in the S_0 state of 5421 ± 8 cm^{-1}. The latter point is also exemplified by the large increase in the intermolecular stretch over the values of 176 cm^{-1} in the S_1 state[136] and the value of 162 cm^{-1} in the S_0 state obtained by dispersed fluorescence spectroscopy.[169] Additionally, between the latter components, another set of progressions of the intermolecular mode of 34 cm^{-1} were seen, this time in combination with a third intermolecular mode of 52 cm^{-1}.

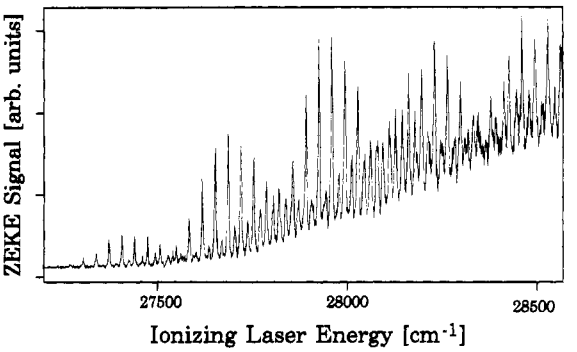

Figure 16. ZEKE spectrum of phenol–methanol via the vibrationless S_1 origin. (Taken from ref 136.)

The ZEKE spectrum obtained via the S_1 state with one quantum of the lowest intermolecular mode, denoted ξ_1, excited, was rather noisy, but still showed the same vibrations as that exhibited by the former ZEKE spectrum. Interestingly, the Franck–Condon envelope had changed substantially (see Figure 17a), which allowed the identification of a fourth intermolecular mode, denoted η_4, at 153 cm^{-1}. A slightly different envelope of the 34 cm^{-1} vibration was also obtained when exciting through the S_1 state with one quantum of the intermolecular stretch (σ) excited. A notable point is that the first band in all these spectra corresponded to the same total laser energy, with respect to the vibrationless ground state—thus indicating that the adiabatic ionization energy had been identified unambiguously. The other two intermolecular modes of the Ph–MeOH cationic complex were identified from the ZEKE spectrum obtained via a combination band (see Figure 17b); their values are 76 and 158 cm^{-1}. Thus, all six intermolecular modes of the cationic complex were identified by using different intermolecular vibrational S_1 levels as intermediate resonances.

Phenol–Ethanol. The third in this series of phenol–X compounds, the Ph–EtOH complex, was also studied in a similar manner to the two described

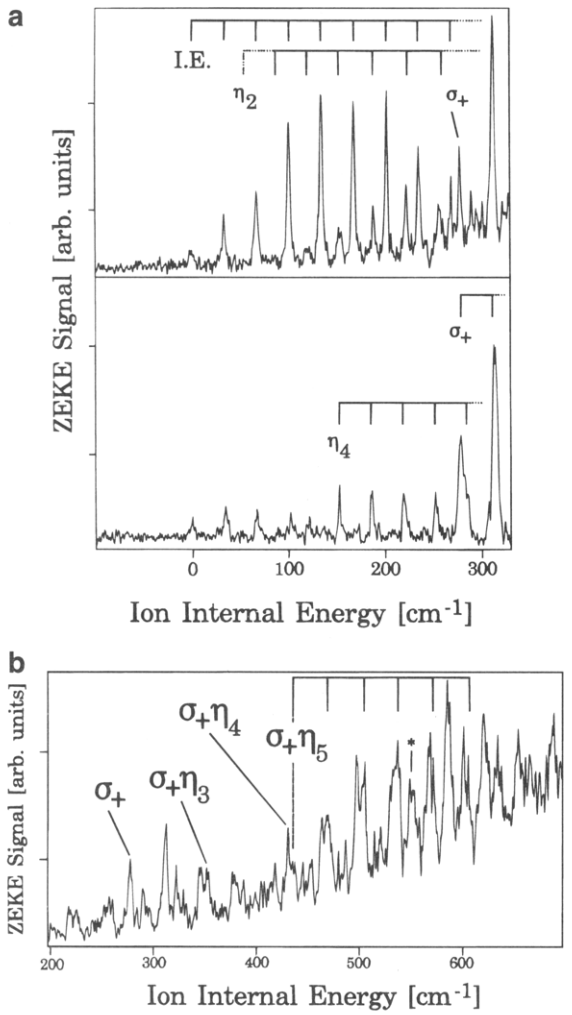

Figure 17. ZEKE spectra of the phenol−methanol complex (taken from ref 136). Part a is the expanded view of the origin region of Figure 16 (top), together with the same region of the ZEKE spectrum obtained via the $S_1\xi_1$ intermediate level (bottom). Of note is the different FC envelope of the intermolecular vibrational pattern allowing the determination of the η_4 *vibration*. Part b is the expanded view of the origin region of the spectrum obtained when exciting through the intermolecular S_1 $\xi_3^1\xi_1'^1$ vibrational level, showing the η_3 and η_5 vibration. In both parts of this figure, the "combs" represent η_1 progressions on the different vibrational origins.

above. The 1 + 1′ REMPI spectrum had been recorded previously by Lipert and Colson[170] as part of their hole-burning study. In this study, the low-frequency region of the REMPI spectrum, corresponding to the $S_1 \leftarrow S_0$ transition, was interpreted in terms of three vibrations of 15, 19, and 26 cm^{-1}. This was a reinterpretation over that of Abe *et al.*[142] who interpreted this region of the spectrum in terms of two rotational isomers; however, the hole-burning experiment was conclusive in showing that only one isomer of Ph−EtOH contributed to this region of the spectrum. The interpretation of the 1 + 1′ REMPI spectrum presented in ref 137 agreed with that of ref 170, and indeed confirmed it, as other combination bands of the aforementioned fundamentals were seen. Also in ref 137, the intermolecular stretch of the S_1 state was observed at 162 cm^{-1}. ZEKE spectra were again recorded via different vibrational levels of the S_1 state. The spectrum recorded via the vibrationless level showed a well-resolved spectrum

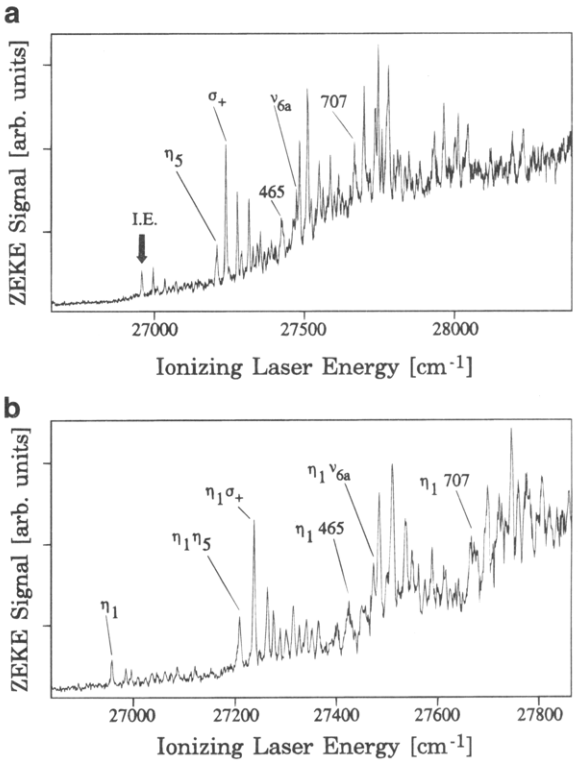

Figure 18. ZEKE spectra of the phenol−ethanol complex via (a) the S_1 origin and (b) via the intermolecular S_1 ξ_3 level. Of note is that the whole FC pattern in b has shifted by the frequency of η_1 compared to a. (Taken from ref 137.)

(see Figure 18a) that exhibited, once again, a progression of the intermolecular stretch. The frequency was 279 cm^{-1} and again indicated a large increase over that of the S_1 state (*vide supra*) and the S_0 state (153 cm^{-1}).[169] The AIE was determined as 62901 ± 5 cm^{-1}, an increase in binding energy of 5727 ± 10 cm^{-1} over that in the S_0 state. The ZEKE spectra obtained, again by exciting through the different S_1 vibrational levels (see Figure 18), led to the identification of all six intermolecular vibrations of the Ph−EtOH cation. Apart from the intermolecular stretch, these are 25, 38, 53, 107, and 248 cm^{-1}. Particularly striking is the fact that in the ZEKE spectrum via the S_1 ξ_3 level (Figure 18b) the whole FC pattern is shifted by the frequency of η_1 compared to the S_1 origin ZEKE spectrum (Figure 18a).

Interestingly, whereas in the cases of Ph−H_2O and Ph−MeOH complexes structured ZEKE spectra were obtained when exciting through the S_1 state with one quantum of the intermolecular stretch excited, for the Ph−EtOH complex, a spectrum almost totally void of structure was obtained. This was attributed to rapid intramolecular (intracomplex) vibrational relaxation (IVR) in the S_1 state—a similar conclusion was reached for the lack of structure when exciting through the S_1 state with one quantum of the phenol-localized ν_{6a} vibration excited.[136] Interestingly, the phenol−water complex showed structured spectra when the ν_{6a} and the ν_{12} vibrations were excited.[171] There is obviously a critical dependence of the IVR rate on the density of the intermolecular vibrational states that can act as a bath for the vibrational energy in these complexes. In fact, Ito and coworkers[172] had shown that even for quite small amounts of excess energies (*ca.* 100 cm^{-1}), the IVR

rate is rather rapid in these complexes. In the similar case of the *p*-alkoxybenzenes,[173] IVR was also seen to be rapid—an indirect measurement[174] of the rate, by looking at the predissociation of Ar and N_2 *p*-alkylbenzene complexes, yielded a value of *ca.* 10^{10} s^{-1}. Further comments on IVR in these species are given in ref 136.

ii. Phenol Dimer

The phenol dimer was studied by Fuke and Kaya[143,175] by 1 + 1 REMPI spectroscopy. In the first paper,[175] two origins were identified in the REMPI spectrum; these correspond to the $S_1 \leftarrow S_0$ ($\pi^* \leftarrow \pi$) transition on each of the proton-donating and proton-accepting phenol rings. Following the conclusions of Ito,[176] the origin shifted to the red of the corresponding transition in isolated phenol (by 303 cm^{-1}) was assigned to the proton-donating moiety, and the one shifted to the blue (by 353 cm^{-1})[143] was assigned to the proton-accepting moiety. Vibrational structure was seen on the proton-donating origin, notably low-frequency modes of 15 and 112 cm^{-1}; these were assigned to an intermolecular bend and the intermolecular stretch; the intermolecular stretch was remeasured as 119.5 cm^{-1} in the later work of Dopfer *et al.*[138] Owing to the presence of other features, shifted by 6 cm^{-1} from the aforementioned ones, it was postulated by Fuke *et al.* that these bands could be due to rotational isomers. In the later study,[138] however, the low-frequency region on the proton-donating origin (denoted S_1^{donor}), was successfully interpreted in terms of one isomer: five vibrations were identified, with frequencies, 7, 11, 14.5, 38.5, and 119.5 cm^{-1}—the latter being the intermolecular stretch. On the $S_1^{acceptor}$ origin, only two modes were identified[138,177] at 9 and 16 cm^{-1}. Note that different intermolecular frequencies are to be expected since the S_1^{donor} and $S_1^{acceptor}$ states are really two different electronic states. In fact it was noted[138] that the $S_1^{acceptor}$ state was really the S_2 state of the complex. Intramolecular modes were seen on the S_1^{donor} origin in the REMPI studies, only one study reported evidence for an intramolecular vibration on the $S_1^{acceptor}$ origin.[143]

REMPI-PES studies were performed[160] in order to ascertain the ionization energy of the phenol dimer. A 1 + 1 REMPI scheme was used, in tandem with energy analysis of the resulting electrons. (The energy of the dye laser was fixed on the relative $S_1 \leftarrow S_0$ transition energy.) The broad, rather featureless band allowed AIEs to be estimated as 8.16 eV for the proton-donating moiety and 8.20 eV for the proton-accepting moiety. It is noted that the phenol trimer REMPI[143] and REMPI-PES[160] spectra were also successfully recorded.

In the ZEKE study[138] of the phenol dimer, a clear vibrational structure was obtained when exciting via the S_1^{donor} origin (see Figure 19), similar to that of the case of phenol–methanol. Analysis of the bands led to vibrational frequencies of 19 and 181 cm^{-1}. These were assigned to an intermolecular bend and the intermolecular stretch of the cation. Broadening in the progressions of the bending vibration led to the conclusion that there could be another almost degenerate vibrational mode of the cation excited upon ionization. Also it could be that there is a vibration of *ca.* 40 or *ca.* 60 cm^{-1} *etc.* that is appearing under the later components of the bend progression. It was not possible to tell from the spectra which possibility was the true one. The ionization energy was not easy to discern unambiguously, owing to poor FCFs in the region of the AIE, but a spectrum recorded exciting through the S_1^{donor} state with one quantum of the 7 cm^{-1} vibration excited allowed a confident determination of the AIE as 63649 ± 4 cm^{-1}. Interestingly, this value is *ca.* 2000 cm^{-1} lower than the value reported by Fuke *et al.*[160] (from the REMPI-PES study), showing the difficulties of determining the AIE when the spectrum is poorly resolved, and the onset is weak. The difference in binding energy between the S_0 state and the proton-donating cation was determined as 4980 cm^{-1}. This increase in binding energy is again reflected in the intermolecular stretch frequency, which increases from 119.5 to 181 cm^{-1} from the S_1^{donor} to the corresponding cation. Attempts to record ZEKE spectra from vibrationally-excited levels of the S_1^{donor} with even very low amounts of internal energy (≥20 cm^{-1}) led to broad, structureless spectra. This was attributed to a combination of poor FCFs and rapid IVR in the S_1^{donor} state. Intriguingly, structureless spectra were also obtained when exciting through the $S_1^{acceptor}$ origin,[138,177] this was attributed to rapid internal conversion between the $S_1^{acceptor}$ and S_1^{donor} states.

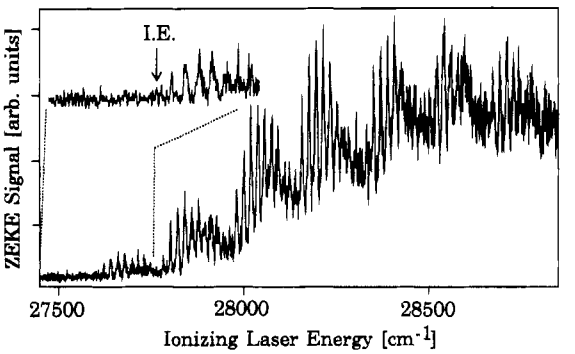

Figure 19. ZEKE spectrum of phenol dimer via the vibrationless S_1 origin. (Taken from ref 138.)

Finally, Felker and co-workers have deduced the most probable structure of the neutral ground state of the phenol dimer complex by analysis of rotational coherence spectra,[178] the most-favored structure is shown in Figure 20. This geometry is different from that thought most likely by other workers.[176,179] Since electron density in the π-ring systems helps to determine the structure of this complex, then it may be seen that when ionization occurs, substantial geometry changes may be expected.

iii. Phenol–Dimethyl Ether

As a comparison with the Ph–H_2O complex, phenol–dimethyl ether (Ph–DME) was chosen, since it too is expected to have C_s symmetry, at least in the ground electronic state, S_0.[180] It was anticipated in the ZEKE study (ref 139) that there would be a symmetry effect, such that only certain intermolecular vibrations would be excited on ionization (*cf.* the difference in the ZEKE spectra between Ph–H_2O and

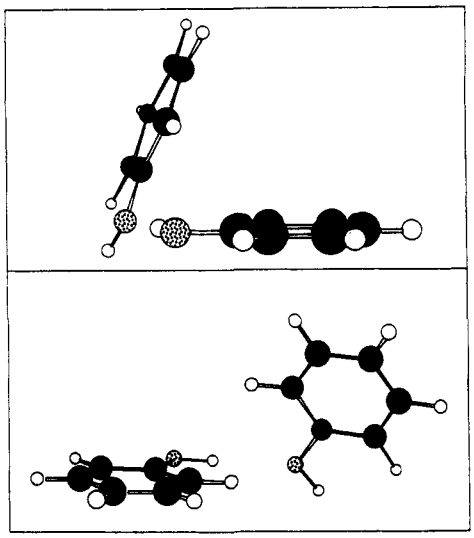

Figure 20. Two views of the most probable structure of the neutral phenol dimer. (Taken from ref 178.)

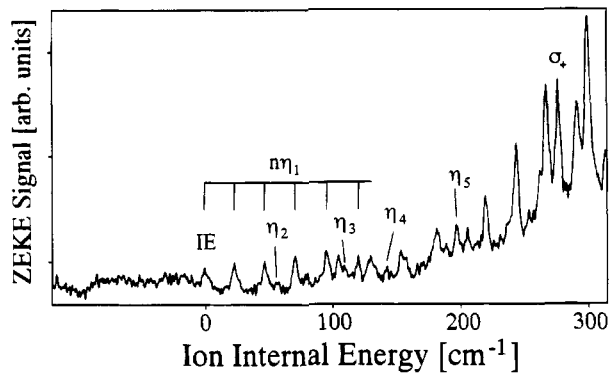

Figure 21. ZEKE spectrum of phenol–dimethyl ether via the vibrationless S_1 origin. The comb indicates the progression of an intermolecular bend vibration, denoted η_1, starting on the ionization energy band (IE). Further η_1 progressions in combination with other intermolecular vibrational fundamentals of the ionic complex [which are denoted η_i ($i = 2-5$) for other bends and the torsion, and σ_+ for the stretch] are observed, but not indicated in the figure in order to avoid congestion. (Taken from ref 139.)

Ph–MeOH). However, the ZEKE spectrum of Ph–EtOH[137] was rather a surprise in that it seemed to show much simpler structure than anticipated. In fact, the Ph–DME ZEKE spectrum turned out to be much more complicated than expected and a "lack of the symmetry effect" was observed.

The Ph–DME complex had been studied previously by infrared spectroscopy[181] and also by LIF spectroscopy.[147] In the latter study, the $S_1 \leftarrow S_0$ transition was examined; there were two peaks in the spectrum separated by 107 cm^{-1} and it was hypothesized that these were due to two different rotational isomers of the Ph–DME complex; however, despite rather thorough precautions to exclude water from the apparatus, it appears from the (mass-resolved) 1 + 1′ REMPI results of ref 139 that the lowest energy feature attributed to Ph–DME in ref 142 is due to a Ph–DME–$(H_2O)_n$ species. Thus the origin of the Ph–DME complex is situated at 35893.6 cm^{-1} and the features seen in the REMPI spectrum are all from one isomer. The ZEKE spectrum recorded via the $S_1 \leftarrow S_0$ origin (see Figure 21) has a very slowly-rising onset but the AIE could be determined at 62604 ± 5 cm^{-1}, representing a large increase in binding energy of 6024 ± 10 cm^{-1}. Again, six intermolecular vibrational origins were identified as 24 (η_1), 57 (η_2), 109 (η_3), 141 (η_4), 196 (η_5), and 275 cm^{-1} (σ_+); the 141 cm^{-1} assignment was made tentatively. The 275 cm^{-1} vibration is the intermolecular stretch and is again a large increase over that in the S_1 state of 141 cm^{-1}. Again, rapid IVR was invoked to explain the lack in structure when exciting through the σ and ν_{6a} vibrations of the S_1 state.

iv. Comparison between the Different Hydrogen-Bonded Phenol–X Complexes

It is clear from Table 3 that the binding energies (of the order of 1 eV) of the hydrogen-bonded complexes are much greater than those of all the other complexes. Again, this is the reason for the strong increase of the intermolecular stretch frequencies in the cations compared to the neutral states. In comparing the binding energies of the hydrogen-bonded, phenol-containing complexes it is noted that the most significant amount of the binding energy change occurs in the $\tilde{X}^+ \leftarrow S_1$ transition and so it is changes in bonding in the cation that are predominant in affecting these values. For example, if the series Ph–H_2O, Ph–MeOH, and Ph–DME is considered, then it may be expected that the hydrogen bond would be getting stronger, owing to the increased electron density on the proton-accepting oxygen atom. (This latter increase comes about since methyl groups are generally electron-pushing groups relative to hydrogen.) In fact, the observed increases in binding energy follow the expected trend with the increases in binding energy on ionization being derived as 4601, 5421, and 6024 cm^{-1}. However, although these values follow the expected trend, this is only generally true of thermodynamic values *obtained in the gas phase*—in solution additional hydrogen bonding to solvent molecules can occur and confuse the issue.[182] Other gas phase studies have also found that substituting methyl groups for hydrogen atoms facilitates bonding, for example, the studies of Millen and co-workers[181,183] on amines, where it was determined that the strength of hydrogen bonding (with various proton donors) followed the order $Me_3N > Me_2NH > MeNH_2$. Similarly, the series Ph–H_2O, Ph–MeOH, and Ph–EtOH may be examined. The increases of binding energy on ionization are 4601, 5421, and 5727 cm^{-1}. The ordering is the same as for the amines[183]—$EtNH_2 > MeNH_2 > NH_3$—from which it may be inferred that the bonding is also increasing in this order. Thus, qualitative arguments work quite well for the bonding in these complexes.

One complex that is difficult to place in this series is the phenol dimer. Felker and co-workers have noted[178] that ring–ring interactions could play an important part of the bonding in this complex, and indeed the progressions of the intermolecular bend observed in the ZEKE spectrum[138] suggest that this is probably true of the cation also.

The changes in cationic intermolecular vibrational frequencies across this series of complexes (summarized in Table 5) is hard to describe even qualitatively. Dopfer *et al.*[184] have noted that this is probably because of the large effect on the vibrations

Table 5. Intermolecular Vibrational Frequencies of the Phenol–X Cations

phenol–X (X =)	observed intermolecular frequencies[f] (cm^{-1})
H_2O[a]	67, 84, ***240***, 257,[g] 328
CH_3OH[b]	34, 52, 76, 153, 158, ***278***
CH_3CH_2OH[c]	25, 38, 53, 107, 248, ***279***
CH_3OCH_3[d]	24, 57, 109, [141], 196, ***275***
C_6H_5OH[e]	19, ***181***

[a] From ref 135. [b] From ref 136. [c] From ref 137. [d] From ref 139. [e] From ref 138. [f] Numbers in bold italic correspond to the intermolecular stretch for each complex. [g] Assigned to the first overtone of the intermolecular torsion (2τ); see ref 135 for details.

of subtle effects of bonding, steric hindrance and the reduced masses of the particular vibrations. It was also noted that help would have to come from the direction of *ab initio* calculations to elucidate the situation further.

v. Intramolecularly Hydrogen-Bonded Species

Only two intramolecular species have been studied to date by ZEKE spectroscopy: tropolone[140,141] and 9-hydroxyphenalenone[141] (hereafter abbreviated as TrO and 9-HPO). These compounds both have a ketone group positioned close to a carbon to which is attached a hydroxy group. Owing to the proximity of the ketonic oxygen, the hydrogen atom on the hydroxy group may tunnel between the two oxygens, in the form of a proton. It is known (*vide infra*) that there are quite different barriers for proton tunneling in the S_0 and S_1 states: the question is, what are the barriers like in the $\tilde{X}^+$ state? There are two opposing factors to the ease of tunneling. Consider first tropolone, TrO has seven carbon atoms and there are thus seven π electrons. In the cation, therefore, there are six π electrons and so the aromaticity criterion is fulfilled. In order for aromaticity to occur, however, the seven-membered ring must be planar—this pushes the oxygens closer together and hence promotes hydrogen bonding. This effect has been termed the "geometric effect" on the tunneling of the proton according to Ozeki *et al.*[140,141] The delocalization of the π electrons also causes a lowering in electron density on the ketonic oxygen and this inhibits the proton tunneling: the "electronic effect". The result of the competition between these two processes determines the tunneling barrier. A similar situation holds with 9-HPO where the outer carbon skeleton has a 10-electron system in the cation.

The S_0 and S_1 states of TrO have been investigated by Redington *et al.*[185] and Sekiya *et al.*[186] and have been estimated to have tunneling splittings of 0.3 and 19 cm^{-1}, respectively. The 1 + 1′ REMPI spectrum[140] clearly showed the tunneling doublets. ZEKE spectra were recorded by exciting via one component and then the other, and the resulting spectra indicated that the first band in each case occurred at the same *total* energy, and thus that there was no observable splitting in the $\tilde{X}^+$ state—*i.e.* it was less than 2 cm^{-1}. (Excitation from either the + or − parity component of the tunneling doublets will lead to population of the same parity component in the cation—if tunneling had occurred in the $\tilde{X}^+$ state, then some splitting would have been observed in the ZEKE spectrum.) The π^{-1} ionization therefore seems to allow electronic effects to dominate over geometric ones. The AIE, corresponding to the lowest-energy peak in the ZEKE spectrum, was obtained as 68365 ± 5 cm^{-1}.

The S_0 state of 9-HPO had been studied previously in a rare gas matrix by Bondybey and co-workers[187] and was found to have a ground state tunneling splitting of 69 cm^{-1}. It was thus not possible to perform a similar experiment to that as for TrO, since the upper component would not have been populated in the jet and hence would not have been seen in the $S_1 \leftarrow S_0$ transition. However, the deuterated analogue (where the hydroxy hydrogen is substituted, denoted 9-HPO-d) has a splitting of 12 cm^{-1}, and it was possible to perform such an experiment. For the 9-HPO-h compound, it was possible to obtain a ZEKE spectrum[141] by exciting through the vibrationless level of the $S_1 \leftarrow S_0$ transition—this gave an AIE of 65338 ± 5 cm^{-1}. For the 9-HPO-d compound, the REMPI spectrum showed two peaks which were assigned to the two tunneling components—they were separated by 179 cm^{-1}. ZEKE spectra were taken via each of these features and these led to two AIEs, differing by 11 cm^{-1}. This difference was attributed to the different tunneling doublets in the S_0 state, in good agreement with the value of 12 cm^{-1} previously obtained by Bondybey *et al.*[187] This implies that the splitting in the $\tilde{X}^+$ state is less than the experimental resolution, and so was $\leq$1 cm^{-1}.

It hence appears that for the two species, the proton tunneling is severely curtailed in the cation states. Since 9-HPO has a rigid skeletal structure, even upon ionization (*cf.* the He I photoelectron spectrum[188]), then, as with TrO, this was attributed to electronic factors, and so the ketonic oxygen is losing some of its electron density to the aromatic π cloud formed in the cation.

IV. Outlook

As is the norm, with an article such as this, the final section usually deals with the authors' ideas on where progress will be concentrated next. This is difficult with the field of research described above since it is expanding so rapidly. Each subsection of species will be considered and some further directions suggested.

For the small complexes it has been shown that vibrational structure is rather easily obtainable, with the increase of experimental resolution to 0.1 cm^{-1} it may be possible to start to resolve rotational structure in some complexes—this will give more accurate cationic complex geometries than has been previously obtained. Also, the work on Xe_2 could be extended by making use of an intermediate state, as was suggested by Tonkyn and White.[63] Similar studies could also be extended to other rare gas dimers, both homogeneous and heterogeneous. Various other small complexes can be envisioned, one that has recently gained attention is the $Ar–I_2$ complex, whose Rydberg spectrum was recently reported by Cockett *et al.*[189] ZEKE spectroscopy of this complex is underway.

Anionic carbon clusters were considered in detail from the work of Neumark and co-workers. This work is still clearly capable of studying other mem-

bers of the C_n^- series. This area is still active. For example, Wurz and Lykke[190] have recently obtained a good, conventional photodetachment spectrum of C_2^-.

It would be interesting to see results on the photoionization of the neutral species also. Recently, Bowers and co-workers have studied the C_7^+ species[191] and Ramanathan *et al.*[192] have bracketed the ionization energies of the C_n species (n = 3–6). Of course, in order to obtain reliable spectra of these species (since one is starting with a neutral species), it is probably necessary to use spectroscopic selection of each particular species. In addition, the AIEs of the species C_3, C_4, and C_5 are rather high (>12 eV) and so an intermediate resonance may be necessary in any case—the AIE of C_6 is lower, at about 9.7 eV.

The work on I^-–CO_2 showed that detailed information may be obtained about neutral complexes (and the anion) by use of the ZEKE variant of photodetachment spectroscopy. There are clearly many clusters to which this could be extended. As examples the following are noted: $H^-(NH_3)$, this has been studied by Coe *et al.*[193] using photodetachment spectroscopy, and it would be interesting to see whether the relatively simple spectrum showed any further structure at the higher resolutions obtained by Neumark and co-workers. The N_2O dimer has been studied[194] by detachment from $(N_2O)_2^-$, the spectrum was rather broad and no structure was identified, some structure was seen in the photodetachment spectrum of N_2O^- and again higher resolution could help to elucidate these systems further; $Cl^-(NH_3)$ has recently been shown to exhibit two main features in its photodetachment spectrum[195] one was assigned to detachment from Cl^- and the other was assigned to a resultant charge-transfer state, $Cl^-NH_3^+$. The latter band showed some structure and it would be very interesting to investigate this in more detail. Very recently, Nakjima *et al.*[196] have looked at the photodetachment spectrum of $(C_6F_6)_n^-$ (n = 1–8) and Au–$C_6F_6^-$ and broad bands were seen in each case. It was noted therein that ZEKE experiments were underway in that group.

There will undoubtedly be more studies on van der Waals complexes containing organic molecules, if only because these are often formed in the jet anyway, and so relatively little effort over that of recording the spectrum of the isolated molecule is needed. The picosecond studies of Knee and co-workers are sure to be extended to other systems helping to probe dynamics of intermediate states. ZEKE spectroscopy is probably more widely applicable than the more commonly used technique of dispersed fluorescence since all molecules and clusters may be ionized, but not all fluoresce. (Also detection of charged particles is much more efficient than photon detection.) It is also noted that femtosecond techniques have already been applied to molecular clusters by Gerber and co-workers[197] and has allowed observation of wavepacket dynamics within the $\tilde{B}$ state of the sodium trimer complex.

With the hydrogen-bonded complexes, it would clearly be of interest to try to record spectra of larger complexes, especially with more solvent ligands attached. Work on the phenol–$(H_2O)_3$ complex is planned at Munich. Other species are also of interest. For example, the benzene–ammonia complex has recently been studied by Rodham *et al.* by REMPI spectroscopy[198] and was of great interest as ammonia was acting as a proton *donor*. It would be of interest to be able to obtain the ZEKE spectrum and also the binding energy in the cation.

Related to the previous suggestions are the possibilities of proton transfer in the ionic state: Mikami *et al.*[199] showed that for the phenol–water complex the proton is not transferred in the ion, whereas for phenol–$(CH_3)_3N$ the proton is transferred.[200] It would be interesting to see what effect this has on the ZEKE spectrum, especially as a function of increasing internal energy. Indeed it could be possible to follow the proton transfer using the picosecond techniques of Knee and co-workers, maybe even extended to femtosecond methods. Recently, fluorescence excitation of tropolone–rare gas complexes have been obtained by Sekiya *et al.*,[201] where it was found that the intermolecular modes and modes involving the transferring proton interact. In the ion, the binding of the rare gas would be expected to be much stronger, and ZEKE spectroscopy would be an ideal way of studying the effects of this interaction on the tunneling dynamics.

Finally it is noted that the related technique of mass-analyzed threshold ionization (MATI), developed by Zhu and Johnson[202] is showing itself to be a powerful technique for looking at complexes. [For MATI, the pulsed-field ionization (PFI) process shown in Figure 1b is used.] Recently work has appeared from the groups of Neusser and Duncan. Neusser and co-workers have concentrated on the benzene–rare gas complexes[203,204] in an effort to understand the van der Waals modes and to determine the dissociation energies of the cationic complexes. Willey *et al.*[205] have studied the Al–Ar complex using the MATI technique. This allowed them to obtain vibrational structure of the cation and (by analyzing hot band structure) of the neutral complex. Not many details are given here regarding the MATI technique as Neusser and co-workers have a companion paper in this issue[206] on this topic, to which readers are directed.

In summary, the ZEKE technique and its companion, MATI, have proved themselves to be extremely versatile and sensitive techniques and will no doubt give a cornucopia of new data in future years, leading to a more in-depth understanding of complex and cluster formation, dynamics, and bonding.

V. Summary

This article is aimed at the review of the plethora of results on various types of clusters and complexes that have been obtained recently by the ZEKE spectroscopic technique. The substantial increase in spectral resolution of *ca.* 2–3 orders of magnitude compared to conventional photoelectron spectroscopy has led to substantial progress in the understanding of intermolecular structure, interactions, and dynamics.

ZEKE spectra of neutral clusters provide accurate data on ionization energies as well as useful informa-

tion about the vibrational structure of the cationic complexes, with the focus mainly on the low-frequency *inter*molecular modes which cannot be observed easily with other techniques. Hence, the intermolecular potential of the ionic complexes can be probed with high resolution and the results can be compared with theoretical approaches. In the case of anthracene–Ar_n clusters it was shown that the sensitivity and resolution of the ZEKE method is sufficient to resolve questions concerning different isomers. The hydrogen-bonded phenol–X complexes (with X being different solvent molecules) served as a model series for studying the *micro*solvation process as a function of the solvent molecule.

In contrast to ZEKE studies of neutral complexes (where mainly properties of the cation clusters are obtained), ZEKE studies on anionic clusters are extremely useful in obtaining information on the corresponding neutral species which are sometimes difficult to prepare selectively (one striking example is the study of the IHI transition state). Of particular note is that these results are to some extent complementary to those obtained by the high-resolution IR technique, for example, totally-symmetric vibrations can be observed.

In addition, it was shown that the ZEKE technique can be used as an ideal probe technique (with high resolution and sensitivity) for monitoring dynamical effects in the intermediate state, like IVR or dissociation, using picosecond or even femtosecond pump–probe schemes. The results are complementary to other probe techniques like for example laser-induced fluorescence.

In summary, the field of ZEKE spectroscopy on complexes and clusters has expanded already to a wide area in the last few years and there will be almost certainly many further applications in the future.

Acknowledgments. The authors thank E. W. Schlag for his support and encouragement while this work was performed. T.G.W. would like to thank the Royal Society for the award of a Postdoctoral fellowship under the European Exchange program for the time he was at Munich. He would also like to thank The Ohio State University (Graduate School) for the award of a Postdoctoral Fellowship for his stay at Columbus, OH. Experimental work of E. Cordes and G. Lembach on the phenol–X clusters is gratefully acknowledged. The authors also thank G. Reiser and S. D. Colson for helpful discussions in the earlier part of these studies. The authors thank D. M. Neumark, M. A. Duncan, K. Kimura, and M. C. R. Cockett for sending reprints and preprints of their work. J. M. Williamson is thanked for reading through the manuscript and making useful suggestions.

References

(1) Hobza, P.; Zahradník, R. *Intermolecular Complexes: The Role of van der Waals Systems in Physical Chemistry and in the Biodisciplines*; Elsevier: Amsterdam, 1988.
(2) Ito, M. *J. Mol. Struct.* **1988**, *177*, 173.
(3) A large number of reviews on this work have been published, see the following and references therein: Ito, M. In *Vibrational Spectra and Structure*; Durig, J. R., Ed.; Elsevier: Amsterdam, 1986; Vol. 15. Ito, M.; Ebata, T.; Mikami, N. *Annu. Rev. Phys. Chem.* **1988**, *39*, 123. Ito, M.; Yamamoto, S.; Aoto, T.; Ebata, T. *J. Mol. Struct.* **1990**, *237*, 105. Gerhards, M.; Kimpfel, B.; Pohl, M.; Schmitt, M.; Kleinermanns, K. *J. Mol. Struct.* **1992**, *270*, 301.
(4) Kebarle, P. *Annu. Rev. Phys. Chem.* **1977**, *28*, 445.
(5) Castleman, A. W., Jr.; Keesee, R. G. *Acc. Chem. Res.* **1986**, *19*, 413.
(6) Delahay, P. *Acc. Chem. Phys.* **1982**, *15*, 40.
(7) Maitland, G. C.; Rigby, M.; Smith, E. B.; Wakeham, W. A. *Intermolecular Forces: Their Origin and Determination*; Clarendon Press: Oxford, 1981.
(8) Topp, M. R. *Int. Rev. Phys. Chem.* **1993**, *12*, 149.
(9) Hutson, J. M. *Annu. Rev. Phys. Chem.* **1990**, *41*, 123. Cohen, R. C.; Saykally, R. J. *Annu. Rev. Phys. Chem.* **1991**, *42*, 369. Cohen, R. C.; Saykally, R. J. *J. Phys. Chem.* **1992**, *96*, 1024.
(10) Hirota, E. *Chem. Rev.* **1992**, *92*, 141.
(11) Rao, C. N. R.; Pradeep, T. *Chem. Soc. Rev.* **1991**, *20*, 477.
(12) Tomoda, S.; Kimura, K. In *Photoionization and Photodissociation of Small Molecules and Clusters*; Ng, C. Y., Ed.; World Scientific: Singapore, 1991.
(13) Hillier, I. H. In *Molecular Interactions*; Ratajczah, H., Orville-Thomas, W. J., Eds.; John Wiley and Sons: New York, 1981; Vol. 2, p 493.
(14) Peel, J. B.; Willett, G. D. *J. Chem. Soc., Faraday Trans. 2* **1975**, *71*, 1799.
(15) Ervin, K. M.; Lineberger, W. C. In *Advances in Gas Phase Ion Chemistry*; Adams, N., Babcock, L. M., Eds.; JAI Press: London, 1992; Vol. 1.
(16) Müller-Dethlefs, K.; Schlag, E. W. *Annu. Rev. Phys. Chem.* **1991**, *42*, 109.
(17) Schlag, E. W.; Peatman, W. B.; Müller-Dethlefs, K. *J. Electron Spectrosc. Relat. Phenom.* **1993**, *66*, 139.
(18) Grant, E. R.; White, M. G. *Nature* **1991**, *354*, 249. Pratt, S. T.; Dehmer, P. M.; Dehmer, J. L.; McCormack, E. F. *Comments At. Mol. Phys.* **1993**, *28*, 259. Wright, T. G.; Reiser, G. F.; Müller-Dethlefs, K. *Chem. Brit.* **1994**, *30*, 128.
(19) Müller-Dethlefs, K.; Sander, M.; Schlag, E. W. *Z. Naturforsch. A* **1984**, *39*, 1089. Müller-Dethlefs, K.; Sander, M.; Schlag, E. W. *Chem. Phys. Lett.* **1984**, *112*, 291.
(20) Reiser, G.; Habenicht, W.; Müller-Dethlefs, K.; Schlag, E. W. *Chem. Phys. Lett.* **1988**, *152*, 119.
(21) Merkt, F.; Softley, T. P. *Phys. Rev. A* **1992**, *46*, 302. Wilson, S. H. S.; Rednall, R. J.; Fielding, H. H.; Merkt, F.; Softley, T. P. *J. Electron Spectrosc. Relat. Phenom.* **1993**, *66*, 151.
(22) Merkt, F.; Softley, T. P. *Int. Rev. Phys. Chem.* **1993**, *12*, 205.
(23) Chupka, W. A. *J. Chem. Phys.* **1993**, *98*, 4520. Chupka, W. A. *J. Chem. Phys.* **1993**, *99*, 5800.
(24) Merkt, F.; Fielding, H. H.; Softley, T. P. *Chem. Phys. Lett.* **1993**, *202*, 153.
(25) Merkt, F.; Zare, R. N. *J. Chem. Phys.*, submitted for publication.
(26) Even, U.; Ben-Nun, M.; Levine, R. D. *Chem. Phys. Lett.* **1993**, *210*, 416.
(27) Pratt, S. T. *J. Chem. Phys.* **1993**, *98*, 9241.
(28) Merkt, F. *J. Chem. Phys.* **1994**, *100*, 2623.
(29) Dietrich, H.-J.; Lindner, R.; Müller-Dethlefs, K. *J. Chem. Phys.* **1994**, *101*, 3399. Lindner, R.; Dietrich, H.-J.; Müller-Dethlefs, K. *Chem. Phys. Lett.*, submitted for publication. Fischer, I.; Lindner, R.; Müller-Dethlefs, K. *J. Chem. Soc., Faraday Trans.* **1994**, in press.
(30) Mills, P. D. A.; Western, C. M.; Howard, B. J. *J. Phys. Chem.* **1986**, *90*, 4961; **1986**, *90*, 3331.
(31) Takahashi, M. *J. Chem. Phys.* **1992**, *96*, 2594.
(32) Kimura, K.; Takahashi, M. Optical Methods for Time- and State-Resolved Chemistry. *SPIE Proceedings Series* **1992**, *1638*, 216. *NOTE*: Figure 10 of that work was attributed to the ZEKE spectrum obtained when exciting through the vibrationless $\tilde{C}$ state; however, ref 31 indicates that this was in fact the $\tilde{C}$ state, but with one quantum of the intermolecular stretch excited.
(33) The notation of the term symbol for the NO moiety, with a tilde over it, for the molecular complex, follows the nomenclature used in laser-induced fluorescence; see the two recent reviews by Heaven: Heaven, M. C. *Annu. Rev. Phys. Chem.* **1992**, *43*, 283; *J. Phys. Chem.* **1993**, *97*, 8567.
(34) REMPI (resonance-enhanced multiphoton ionization) spectroscopy accesses an electronically-excited state of a molecule or complex using m photons and then absorption of a further n photons of the same color causes ionization. The process is then known as an $m + n$ REMPI process; if the colors of the photons are different, then the process is known as an $m + n'$ REMPI process.
(35) Sato, K.; Achiba, Y.; Kimura, K. *J. Chem. Phys.* **1984**, *81*, 57.
(36) Miller, J. C.; Cheng, W.-C. *J. Phys. Chem.* **1985**, *89*, 1647.
(37) Note that in ref 31 an error has occurred and the anharmonicities reported are actually twice the value they should be.
(38) Duschinsky, F. *Acta Physiochem. U.R.S.S.* **1937**, *1*, 551. Small, G. J. *J. Chem. Phys.* **1971**, *54*, 3300.
(39) Wright, T. G.; Špirko, V.; Hobza, P. *J. Chem. Phys.* **1994**, *100*, 5403.
(40) Robbe, J.-M.; Bencheikh, M.; Flament, J.-P. *Chem. Phys. Lett.* **1993**, *210*, 170.

(41) Size consistency in an *ab initio* calculation implies that the energy of the complex, when there is infinite separation between the components, is equal to the sum of the energies of the separate components.
(42) The abbreviation HF implies the use of Hartree–Fock theory with the basis set indicated: Hartree, D. R. *Proc. Cambridge Philos. Soc.* **1928**, *24*, 89. Fock, V. *Z. Phys.* **1930**, *61*, 126. Roothaan, C. C. J. *Rev. Mod. Phys.* **1951**, *23*, 161. The abbreviation MP2 implies the use of Møller–Plesset perturbation theory to second order: Møller, C.; Plesset, M. S. *Phys. Rev.* **1934**, *40*, 618. The abbreviation QCISD(T) implies the use of the quadratic configuration method, including single and double excitations and incorporating a perturbative correction for triple excitations: Pople, J. A.; Head-Gordon, M.; Raghavachari, K. *J. Chem. Phys.* **1987**, *87*, 5968.
(43) Miescher, E. *Can. J. Phys.* **1976**, *54*, 2074.
(44) Ferguson, E. E.; Fehsenfeld, F. C.; Albritton, D. L. In *Gas Phase Ion Chemistry*; Bowers, M. T., Ed.; Academic Press: New York, 1979; Vol. 1.
(45) Western, C. M.; Langridge-Smith, P. R. R.; Howard, B. J.; Novick, S. E. *Mol. Phys.* **1981**, *44*, 145.
(46) Kukolich, S. G. *J. Am. Chem. Soc.* **1982**, *104*, 4715.
(47) Menoux, V.; Le Doucen, R.; Haeusler, C.; Deroche, J. C. *Can. J. Phys.* **1984**, *62*, 322 (in French).
(48) Durig, J. R.; Griffin, M. G. *J. Raman Spectrosc.* **1976**, *5*, 273.
(49) Legay, F.; Legay-Sommaire, N. *Chem. Phys. Lett.* **1993**, *211*, 516.
(50) Ha, T.-K. *Theoret. Chim. Acta* **1981**, *58*, 125.
(51) Fischer, I.; Strobel, A.; Staecker, J.; Niedner-Schatteburg, G.; Müller-Dethlefs, K.; Bondybey, V. E. *J. Chem. Phys.* **1992**, *96*, 7171.
(52) Ng, C. Y.; Tiedemann, P. W.; Mahan, B. H.; Lee, Y. T. *J. Chem. Phys.* **1977**, *66*, 3985.
(53) Harrington, J. E.; Weisshaar, J. C. *J. Chem. Phys.* **1990**, *93*, 854.
(54) Cai, M. F.; Dzugan, T. P.; Bondybey, V. E. *Chem. Phys. Lett.* **1989**, *155*, 430.
(55) Cai, M. F.; Carter, C. C.; Miller, T. A.; Bondybey, V. E. *Chem. Phys.* **1991**, *153*, 233.
(56) Sunil, K. K.; Jordan, K. D. *J. Phys. Chem.* **1988**, *92*, 2774.
(57) Bauschlicher, C. W.; Barnes, L. A.; Taylor, P. R. *J. Phys. Chem.* **1989**, *93*, 2932.
(58) Lias, S. G.; Bartmess, J. E.; Liebman, J. F.; Holmes, J. L.; Levin, R. D.; Mallard, W. G. Gas Phase Ion and Neutral Thermochemistry. *J. Phys. Chem. Ref. Data* **1988**, *17*, Suppl. 1.
(59) Fu, Z.; Lemire, G. W.; Bishea, G. A.; Morse, M. D. *J. Chem. Phys.* **1990**, *93*, 8420.
(60) Ng, C. Y. *Adv. Chem. Phys.* **1983**, *52*, 263.
(61) Ma, N. L.; Li, W.-L.; Ng, C. Y. *J. Chem. Phys.* **1993**, *99*, 3617.
(62) Curtiss, L. A.; Raghavachari, K.; Truck, G. W.; Pople, J. A. *J. Chem. Phys.* **1991**, *94*, 2221.
(63) Tonkyn, R. G.; White, M. G. *J. Chem. Phys.* **1991**, *95*, 5582.
(64) Descriptions of the experimental procedure to produce this radiation for use in ZEKE experiments are given in: Tonkyn, R. G.; White, M. G. *Rev. Sci. Instrum.* **1989**, *60*, 1245. Fielding, H. H.; Softley, T. P.; Merkt, F. *Chem. Phys.* **1991**, *155*, 257.
(65) Pratt, S. T.; Dehmer, P. M.; Dehmer, J. L. *J. Chem. Phys.* **1989**, *90*, 2201.
(66) Ng, C. Y.; Trevor, D. J.; Mahan, B. H.; Lee, Y. T. *J. Chem. Phys.* **1976**, *65*, 4327.
(67) Kitsopoulos, T. N.; Waller, I. M.; Loeser, J. G.; Neumark, D. M. *Chem. Phys. Lett.* **1989**, *159*, 300.
(68) Gantefor, G. F. Private communication.
(69) Markovich, G.; Giniger, R.; Levin, M.; Cheshnovsky, O. *J. Chem. Phys.* **1991**, *95*, 9416.
(70) Markovich, G.; Pollack, S.; Giniger, R.; Cheshnovsky, O. *Z. Phys. D: At., Mol. Clusters* **1993**, *26*, 98.
(71) Markovich, G.; Giniger, R.; Levin, M.; Cheshnovsky, O. *Z. Phys. D: At., Mol. Clusters* **1991**, *20*, 69.
(72) Arnold, D. W.; Bradforth, S. E.; Kim, E. H.; Neumark, D. M. *J. Chem. Phys.* **1992**, *97*, 9468.
(73) Cyr, D. M.; Scarton, G.; Johnson, M. A. *J. Chem. Phys.* **1993**, *99*, 4869.
(74) Zhao, Y.; Arnold, C. C.; Neumark, D. M. *J. Chem. Soc., Faraday Trans.* **1993**, *89*, 1449.
(75) Kruit, P.; Read, F. H. *J. Phys. E* **1983**, *16*, 313.
(76) Gantefor, G. F.; Cox, D. M.; Kaldor, A. *J. Chem. Phys.* **1990**, *93*, 8395.
(77) Gantefor, G. F.; Cox, D. M.; Kaldor, A. *Z. Phys. D: At., Mol. Clusters* **1991**, *19*, 59.
(78) Gantefor, G. F.; Cox, D. M.; Kaldor, A. *J. Chem. Phys.* **1992**, *96*, 4102.
(79) Walch, S. P.; Bauschlicher, C. W.; Langhoff, S. R. *J. Chem. Phys.* **1986**, *85*, 5900.
(80) Moskovits, M. *Annu. Rev. Phys. Chem.* **1991**, *42*, 465. Parent, D. C.; Anderson, S. L. *Chem. Rev.* **1992**, *92*, 1541. de Heer, W. A. *Rev. Mod. Phys.* **1993**, *65*, 611.
(81) Weltner, W., Jr.; van Zee, R. J. *Chem. Rev.* **1989**, *89*, 1713.
(82) Arnold, D. W.; Bradforth, S. E.; Kitsopoulos, T. N.; Neumark, D. M. *J. Chem. Phys.* **1991**, *95*, 8753.
(83) Arnold, C. C.; Zhao, Y.; Kitsopoulos, T. N.; Neumark, D. M. *J. Chem. Phys.* **1992**, *97*, 6121.
(84) Gaumet, J. J.; Wakisaka, A.; Shimizu, Y.; Tamori, Y. *J. Chem. Soc., Faraday Trans.* **1993**, *89*, 1667.
(85) Yang, S. H.; Pettiette, C. L.; Conceicao, J.; Chesnovsky, O.; Smalley, R. E. *Chem. Phys. Lett.* **1987**, *139*, 233.
(86) Yang, S.; Taylor, K. J.; Craycroft, M. J.; Conceicao, J.; Pettiette, C. L.; Chesnovsky, O.; Smalley, R. E. *Chem. Phys. Lett.* **1988**, *144*, 431.
(87) Kitsopoulos, T. N.; Chick, C. J.; Zhao, Y.; Neumark, D. M. *J. Chem. Phys.* **1991**, *95*, 5479.
(88) Raghavachari, K.; Binkley, J. S. *J. Chem. Phys.* **1987**, *87*, 2191.
(89) This follows from that fact that according to Wigner (Wigner, E. P. *Phys. Rev.* **1948**, *73*, 1003; see also Rau, A. R. P. *Comments At. Mol. Phys.* **1984**, *14*, 285.) the photodetachment cross-section σ, follows the threshold law:

$$\sigma \propto (E_{\text{photon}} - E_{\text{electron affinity}})^{l+1/2}$$

Since this implies that for $l \neq 0$ the cross section is small very close to threshold, which is the region probed by the ZEKE photodetachment experiment, then it is clear that only *s* waves will contribute to the ZEKE spectrum.
(90) Reed, K. J.; Zimmerman, A. H.; Andersen, H. C.; Brauman, J. I. *J. Chem. Phys.* **1976**, *64*, 1368.
(91) Pacchioni, G.; Koutecký, J. *J. Chem. Phys.* **1988**, *88*, 1066.
(92) Martin, J. M. L.; François, J. P.; Gijbels, R. *J. Chem. Phys.* **1990**, *93*, 8850; *J. Comput. Chem.* **1991**, *12*, 52.
(93) Nimlos, M. R.; Harding, L. B.; Ellison, G. B. *J. Chem. Phys.* **1987**, *87*, 5116.
(94) Douglas, A. E. *Can. J. Phys.* **1955**, *33*, 801.
(95) Van Zee, R. J.; Ferrante, R. F.; Weltner, W., Jr. *J. Chem. Phys.* **1985**, *83*, 6181.
(96) Kitsopoulos, T. N.; Chick, C. J.; Zhao, Y.; Neumark, D. M. *J. Chem. Phys.* **1991**, *95*, 1441.
(97) Arnold, C. A.; Kitsopoulos, T. N.; Neumark, D. M. *J. Chem. Phys.* **1993**, *99*, 766.
(98) Note that in ref 97 a misprint has occurred, and the B_1 peak should be assigned to the $X^3\Sigma_g^- \leftarrow {}^2\Pi_{3/2u}$ ($v'' = 1$) transition: this is correctly designated in ref 96.
(99) Raghavachari, K.; Rohlfing, C. M. *J. Chem. Phys.* **1991**, *94*, 3670.
(100) Cheshnovsky, O.; Yang, S. H.; Pettiette, C. L.; Craycraft, M. J.; Liu, Y.; Smalley, R. E. *Chem. Phys. Lett.* **1987**, *138*, 119.
(101) Kitsopoulos, T. N.; Chick, C. J.; Weaver, A.; Neumark, D. M. *J. Chem. Phys.* **1990**, *93*, 6108.
(102) Arnold, C. C.; Neumark, D. M. *J. Chem. Phys.* **1994**, *100*, 1797.
(103) Rohlfing, C. M.; Raghavachari, K. *J. Chem. Phys.* **1992**, *96*, 2114.
(104) Dixon, D. A.; Gole, J. L. *Chem. Phys. Lett.* **1992**, *188*, 560. Fournier, R.; Sinnott, S. B.; DePristo, A. *J. Chem. Phys.* **1992**, *97*, 4149.
(105) Arnold, C. C.; Neumark, D. *J. Chem. Phys.* **1993**, *99*, 3353.
(106) For recent reviews of work in this area, see: Neumark, D. M. *Annu. Rev. Phys. Chem.* **1992**, *43*, 153. Metz, R. B.; Bradforth, S. E.; Neumark, D. M. *Adv. Chem. Phys.* **1992**, *81*, 1. Neumark, D. M. *Acc. Chem. Res.* **1993**, *26*, 33.
(107) Metz, R. B.; Kitsopoulos, T. N.; Weaver, A.; Neumark, D. M. *J. Chem. Phys.* **1988**, *88*, 1463.
(108) Weaver, A.; Metz, R. B.; Bradforth, S. E.; Neumark, D. M. *J. Phys. Chem.* **1988**, *92*, 5558.
(109) Metz, R. B.; Weaver, A.; Bradforth, S. E.; Kitsopoulos, T. N.; Neumark, D. M. *J. Phys. Chem.* **1990**, *94*, 1377.
(110) Weaver, A.; Neumark, D. M. *Faraday Discuss. Chem. Soc.* **1991**, *91*, 5. Bradforth, S. E.; Arnold, D. W.; Neumark, D. M.; Manolopoulos, D. E. *J. Chem. Phys.* **1993**, *99*, 6345.
(111) Klepeis, N. E.; East, A. L. L.; Császár, A. G.; Allen, W. D.; Lee, T. J.; Schwenke, D. W. *J. Chem. Phys.* **1993**, *99*, 3865.
(112) Waller, I. M.; Kitsopoulos, T. N.; Neumark, D. M. *J. Phys. Chem.* **1990**, *94*, 2240.
(113) Schatz, G. C.; Florance, S.; Lee, T. J.; Bauschlicher, C. W., Jr. *Chem. Phys. Lett.* **1993**, *202*, 495.
(114) Ellison, C. M.; Ault, B. S. *J. Phys. Chem.* **1979**, *83*, 832.
(115) See references quoted in ref 108.
(116) Metz, R. B.; Neumark, D. M. *J. Chem. Phys.* **1992**, *97*, 962.
(117) Chewter, L. A.; Müller-Dethlefs, K.; Schlag, E. W. *Chem. Phys. Lett.* **1987**, *135*, 219.
(118) Chewter, L. A.; Sander, M.; Müller-Dethlefs, K.; Schlag, E. W. *J. Chem. Phys.* **1987**, *86*, 4737.
(119) Rieger, D. Diplomarbeit 1990, Technische Universität, München.
(120) Cockett, M. C. R.; Okuyama, K.; Kimura, K. *J. Chem. Phys.* **1992**, *97*, 4679.
(121) Yamamoto, S.; Okuyama, K.; Mikami, N.; Ito, M. *Chem. Phys. Lett.* **1986**, *125*, 1.
(122) Dyke, J. M.; Ozeki, H.; Takahashi, M.; Cockett, M. C. R.; Kimura, K. *J. Chem. Phys.* **1992**, *97*, 8926.
(123) Lu, K.-T.; Eiden, G. C.; Weisshaar, J. C. *J. Phys. Chem.* **1992**, *96*, 9742.
(124) Lu, K.-T.; Weisshaar, J. C. *J. Chem. Phys.* **1993**, *99*, 4247.
(125) Zhang, X.; Smith, J. M.; Knee, J. L. *J. Chem. Phys.* **1992**, *97*, 2843.
(126) Smith, J. M.; Zhang, X.; Knee, J. L. *J. Chem. Phys.* **1993**, *99*, 2550.

(127) Takahashi, M.; Ozeki, H.; Kimura, K. *J. Chem. Phys.* **1992**, *96*, 6399.
(128) Song, X.; Tang, M.; Davidson, E. R.; Reilly, J. P. *J. Chem. Phys.* **1993**, *99*, 3224.
(129) Bieske, E. J.; Rainbird, M. W.; Knight, A. E. W. *J. Chem. Phys.* **1991**, *94*, 7019.
(130) Nimlos, M. R.; Young, A.; Bernstein, E. R.; Kelley, D. F. *J. Chem. Phys.* **1989**, *91*, 5268.
(131) Bernstein, E. R.; Law, K.; Schauer, M. *J. Chem. Phys.* **1984**, *80*, 634.
(132) Cockett, M. C. R.; Kimura, K. *J. Chem. Phys.* **1994**, *100*, 3429.
(133) Reiser, G.; Dopfer, O.; Lindner, R.; Henri, G.; Müller-Dethlefs, K.; Schlag, E. W.; Colson, S. D. *Chem. Phys. Lett.* **1991**, *181*, 1.
(134) Dopfer, O.; Reiser, G.; Lindner, R.; Müller-Dethlefs, K. *Ber. Bunsen-Ges. Phys. Chem.* **1992**, *96*, 1259.
(135) Dopfer, O.; Reiser, G.; Müller-Dethlefs, K.; Schlag, E. W.; Colson, S. D. *J. Chem. Phys.* **1994**, *101*, 974.
(136) Wright, T. G.; Cordes, E.; Dopfer, O.; Müller-Dethlefs, K. *J. Chem. Soc., Faraday Trans.* **1993**, *89*, 1609.
(137) Cordes, E.; Dopfer, O.; Wright, T. G.; Müller-Dethlefs, K. *J. Phys. Chem.* **1993**, *97*, 7471.
(138) Dopfer, O.; Lembach, G.; Wright, T. G.; Müller-Dethlefs, K. *J. Chem. Phys.* **1993**, *98*, 1933.
(139) Dopfer, O.; Wright, T. G.; Cordes, E.; Müller-Dethlefs, K. *J. Am. Chem. Soc.* **1994**, *116*, 5880.
(140) Ozeki, H.; Takahashi, M.; Okuyama, K.; Kimura, K. *J. Chem. Phys.* **1991**, *95*, 9401.
(141) Ozeki, H.; Takahashi, M.; Okuyama, K.; Kimura, K. *J. Chem. Phys.* **1993**, *99*, 56.
(142) Abe, H.; Mikami, N.; Ito, M. *J. Phys. Chem.* **1982**, *86*, 1768.
(143) Fuke, K.; Kaya, K. *Chem. Phys. Lett.* **1983**, *94*, 97.
(144) Lipert, R. J.; Colson, S. D. *J. Chem. Phys.* **1988**, *89*, 4579.
(145) Lipert, R. J.; Colson, S. D. *J. Phys. Chem.* **1989**, *93*, 135.
(146) Stanley, R. J.; Castleman, A. W., Jr. *J. Phys. Chem.* **1991**, *94*, 7744.
(147) Schütz, M.; Bürgi, T.; Leutwyler, S.; Fischer, T. *J. Chem. Phys.* **1993**, *98*, 3763.
(148) Dopfer, O.; *et al.* To be published.
(149) Oikawa, A.; Abe, H.; Mikami, N.; Ito, M. *J. Phys. Chem.* **1983**, *87*, 5083.
(150) Ebata, T.; Furukawa, M.; Suzuki, T.; Ito, M. *J. Opt. Soc. Am. B* **1990**, *7*, 1890.
(151) Goto, A.; Fujii, M.; Mikami, N.; Ito, M. *J. Phys. Chem.* **1986**, *90*, 2370.
(152) Lipert, R. J.; Colson, S. D. *Chem. Phys. Lett.* **1989**, *161*, 303. Schmitt, M.; Müller, H.; Kleinermanns, K. *Chem. Phys. Lett.* **1994**, *218*, 246.
(153) Stanley, R. J.; Castelman, A. W., Jr. *J. Chem. Phys.* **1993**, *98*, 796.
(154) Hartland, G. V.; Henson, B. F.; Venturo, V. A.; Felker, P. M. *J. Phys. Chem.* **1992**, *96*, 1164.
(155) Ito, M.; Suzuki, T.; Furukawa, M.; Ebata, T. In *Dynamics of Polyatomic Van der Waals Complexes*; Halberstadt, N., Janda, K. C., Eds.; Plenum Press: New York, 1990.
(156) Schütz, M.; Bürgi, T.; Leutwyler, S. *J. Mol. Struct. (THEOCHEM)* **1992**, *276*, 117.
(157) Feller, D.; Feyereisen, M. W. *J. Comput. Chem.* **1993**, *14*, 1027.
(158) Hobza, P.; Burcl, R.; Špirko, V.; Dopfer, O.; Müller-Dethlefs, K.; Schlag, E. W. *J. Chem. Phys.* **1994**, *101*, 990.
(159) Martinez, S. J., III; Alfano, J. C.; Levy, D. H. *J. Mol. Spectrosc.* **1992**, *152*, 80.
(160) Fuke, K.; Yoshiuchi, H.; Kaya, K.; Achiba, Y.; Sato, K.; Kimura, K. *Chem. Phys. Lett.* **1984**, *108*, 179.
(161) Mikami, N.; Sato, S.; Ishigaki, M. *Chem. Phys. Lett.* **1993**, *202*, 431.
(162) Takahashi, M.; Kimura, K. In *Time Resolved Vibrational Spectroscopy V*; Takahashi, H., Ed.; Springer Proc. in Phys. Vol. 68; Springer Verlag: Berlin, 1992.
(163) Lipert, R. J.; Colson, S. D. *J. Chem. Phys.* **1990**, *92*, 3240.
(164) See ref 23 for a discussion on how the proportionality constant can differ from 6.1.
(165) Lembach, G. Diplomarbeit 1992, Technische Universität, München. Lembach, G.; *et al.* To be published.
(166) Gonohe, N.; Abe, N.; Mikami, N.; Ito, M. *J. Phys. Chem.* **1985**, *89*, 3642.
(167) Appel, I.; Kleinermanns, K. *Ber. Bunsen-Ges. Phys. Chem.* **1987**, *91*, 140. Pohl, M.; Schmitt, M.; Kleinermanns, K. *Chem. Phys. Lett.* **1991**, *177*, 252.
(168) For the hydrogen-bonded complexes Ph−MeOH, Ph−EtOH, Ph−DME, and Ph_2 the following nomenclature has been used for the six intermolecular vibrations: ξ_i for bends and the torsion ($i = 1-5$) and σ for the stretch in the S_1 state; η_i for bends and the torsion ($i = 1-5$) and σ_+ for the stretch in the ionic ground state.
(169) Abe, H.; Mikami, N.; Ito, M.; Udagawa, Y. *J. Phys. Chem.* **1982**, *86*, 2567.
(170) Lipert, R. J.; Colson, S. D. *J. Phys. Chem.* **1989**, *93*, 3894.
(171) Dopfer, O.; *et al.* To be published.
(172) Abe, H.; Mikami, N.; Ito, M.; Udagawa, Y. *Chem. Phys. Lett.* **1982**, *93*, 217.
(173) Hopkins, J. B.; Powers, D. E.; Smalley, R. E. *J. Chem. Phys.* **1981**, *74*, 6986.
(174) Hopkins, J. B.; Powers, D. E.; Smalley, R. E. *J. Chem. Phys.* **1981**, *74*, 745.
(175) Fuke, K.; Kaya, K. *Chem. Phys. Lett.* **1982**, *91*, 311.
(176) Ito, M. *J. Mol. Spectrosc.* **1960**, *4*, 125.
(177) It is noted here that in ref 138 an error occurred regarding the assignment of the acceptor origin in the REMPI spectrum. Later experiments with Ne as carrier gas provided colder REMPI spectra with the result that the true acceptor origin must be assigned to a band 9 cm^{-1} lower. (In the previous study this band was assumed to be a hot band.) However, all the main conclusions from ref 138 are still correct and the reassignment will be outlined elsewhere.
(178) Connell, L. L.; Ohline, S. M.; Joireman, P. W.; Corcoran, T. C.; Felker, P. M. *J. Chem. Phys.* **1992**, *96*, 2585.
(179) Bellamy, L. J.; Page, R. J. *Spectrochim. Acta* **1966**, *22*, 525. Remko, M. *Z. Phys. Neue Folge* **1977**, *104*, 177. Moreau Descoings, M. C.; Goethals, G.; Seguin, J. P. *Bull. Chim. Soc. Belg.* **1988**, *97*, 127 (in French).
(180) Cremer, D.; Binkley, J. S.; Pople, J. A.; Hehre, W. A. *J. Am. Chem. Soc.* **1974**, *96*, 6900.
(181) Hussein, M. A.; Millen, D. J.; Mines, G. W. *J. Chem. Soc., Faraday Trans. 2* **1976**, *72*, 686.
(182) For example: Sykes, P. *A Guidebook to Mechanism in Organic Chemistry*; 5th ed.; Longman: New York, 1985.
(183) Hussein, M. A.; Millen, D. J. *J. Chem. Soc., Faraday Trans. 2* **1974**, *70*, 685; 693; **1976**, *72*, 693.
(184) Dopfer, O.; Wright, T. G.; Müller-Dethlefs, K. *J. Electron Spectrosc. Relat. Phenom.* **1994**, *68*, 247.
(185) Redington, R. L.; Redington, T. E. *J. Mol. Spectrosc.* **1979**, *78*, 229. Redington, R. L.; Chen, Y.; Scherer, G. J.; Field, R. W. *J. Chem. Phys.* **1988**, *88*, 627. Redington, R. L. *J. Chem. Phys.* **1990**, *92*, 6447.
(186) Sekiya, H.; Nagashima, Y.; Nishimura, Y. *Bull. Chem. Soc. Jpn.* **1989**, *62*, 3229. Sekiya, H.; Nagashima, Y.; Nishimura, Y. *J. Chem. Phys.* **1990**, *92*, 5761.
(187) Bondybey, V. E.; Haddon, R. C.; English, J. H. *J. Chem. Phys.* **1984**, *80*, 5432.
(188) Song, P.-S.; Latino, M. A. *Bull. Chem. Soc. Jpn.* **1970**, *43*, 278. Carnovale, F.; Gan, T. H.; Peel, J. B.; Franz, K.-D. *Tetrahedron* **1978**, *35*, 129.
(189) Cockett, M. C. R.; Goode, J. G.; Lawley, K. P.; Donovan, R. J. *Chem. Phys. Lett.* **1993**, *214*, 27. Cockett, M. C. R.; Goode, J. G.; Maier, R. R. J.; Lawley, K. P.; Donovan, R. J. *J. Chem. Phys.* **1994**, *101*, 126.
(190) Wurz, P.; Lykke, K. R. *Chem. Phys. Lett.* **1993**, *176*, 185.
(191) von Helden, G.; Gotts, N. G.; Bowers, M. T. *Chem. Phys. Lett.* **1993**, *212*, 241. von Helden, G.; Palke, W. E.; Bowers, M. T. *Chem. Phys. Lett.* **1993**, *212*, 247.
(192) Ramanathan, R.; Zimmerman, J. A.; Eyler, J. R. *J. Chem. Phys.* **1993**, *98*, 7838.
(193) Coe, J. V.; Snodgrass, J. T.; Friedhoff, C. B.; McHugh, K. M.; Bowen, K. H. *J. Chem. Phys.* **1985**, *83*, 3169.
(194) Coe, J. V.; Snodgrass, J. T.; Friedhoff, C. B.; McHugh, K. M.; Bowen, K. H. *Chem. Phys. Lett.* **1986**, *124*, 274.
(195) Markovich, G.; Cheshnovsky, O.; Kaldor, U. *J. Chem. Phys.* **1993**, *99*, 6201.
(196) Nakajima, A.; Taguwa, T.; Hoshino, K.; Sugioka, T.; Naganuma, T.; Ono, F.; Watanabe, K.; Nakao, K.; Konishi, Y.; Kishi, R.; Kaya, K. *Chem. Phys. Lett.* **1993**, *214*, 22.
(197) Baumert, T.; Thalweiser, R.; Gerber, G. *Chem. Phys. Lett.* **1993**, *209*, 29.
(198) Rodham, D. A.; Suzuki, S.; Suenram, R. D.; Lovas, F. J.; Dasgupta, S.; Goddard, W. A., III; Blake, G. A. *Nature* **1993**, *362*, 735.
(199) Mikami, N.; Okabe, A.; Suzuki, I. *J. Phys. Chem.* **1988**, *92*, 1858.
(200) Mikami, N.; Suzuki, I.; Okabe, A. *J. Phys. Chem.* **1987**, *91*, 5242.
(201) Sekiya, H.; Nakajima, T.; Ujita, H.; Tsuji, T.; Ito, S.; Nishimura, Y. *Chem. Phys. Lett.* **1993**, *215*, 499.
(202) Zhu, L.; Johnson, P. *J. Chem. Phys.* **1991**, *94*, 5769.
(203) Krause, H.; Neusser, H. J. *J. Chem. Phys.* **1992**, *97*, 6121; *Chem. Phys. Lett.* **1993**, *213*, 603.
(204) Krause, H.; Neusser, H. J. *J. Chem. Phys.* **1993**, *99*, 6278.
(205) Willey, K. F.; Yeh, C. S.; Duncan, M. A. *Chem. Phys. Lett.* **1993**, *211*, 156.
(206) Neusser, H. J.; Krause, H. *Chem. Rev.* **1994**, *94*, this issue.